A STUDY OF THE FLUORINE PLUS PROTON REACTIONS

Thesis by

Robert Williams Peterson

In Partial Fulfillment of the Requirements

for the Degree of

Doctor of Philosophy

California Institute of Technology

Pasadena, California

1954

ACKNOWLEDGMENTS

The author wishes to express his appreciation to Dr. W. A. Fowler for suggesting and supervising this research, to Drs. Fowler and C. C. Lauritsen for many hours of running the machine, and to Drs. R. F. Christy and A. A. Kraus for illuminating discussions of some of the theoretical aspects of angular distributions.

ABSTRACT

The F^{19} plus proton reactions were studied in an attempt to obtain some information about the energy levels in O^{16} and F^{19}, and indirectly about levels in Ne^{20}.

A high resolution magnetic analysis of the alpha particle groups to the 1^- and 2^+ levels in O^{16} from the $F^{19}(p\,\alpha)O^{16*}$ reaction failed to reveal any doublet structure in these known levels. The angular distributions of the alpha particle groups to the levels did not indicate any degeneracy with a 2^- level, nor did a search for new excited levels in O^{16} up to 9.1 Mev reveal a 2^- level.

Angular distributions of the alpha particles were measured at bombarding energies of 874, 935, 1290, 1355, and 1381 kev. The distributions at 1355 kev indicated that the corresponding Ne^{20} resonance level at 14.23 Mev excitation has spin 2 and odd parity.

A study of the inelastic proton groups from the $F^{19}(p\,p')F^{19*}$ reaction gave 113.9 $\pm$ 0.8 and 199.6 $\pm$ 0.7 kev for the excitation energies of the two lowest known levels of F^{19}. The cross sections at 1431 kev for these groups in the center of mass system were found to be 0.187 $\pm$ 0.015 barns for the first group and 0.007 $\pm$ 0.002 barns for the second group. At 1381 kev, the cross section was found to be 0.0427 $\pm$ 0.0040 barns for protons to the second excited level. Angular distributions were measured where possible, but did not give unique assignments for the levels. However, all distributions obtained were consistent with the assignments made to the levels on the basis of the gamma-ray work done in this laboratory.

TABLE OF CONTENTS

I INTRODUCTION

A study of the F^{19} plus proton reactions was made in an attempt to gain some knowledge of the energy levels of the nuclei involved. The energies of the emitted alpha particle groups ($F^{19}(p\,\alpha)O^{16*}$) reveal energy levels in O^{16}, while the inelastic proton groups ($F^{19}(p\,p')F^{19*}$) determine energy levels in F^{19}. The angular distributions of both the alpha particles and protons are a means of determining the spins and parities of these levels. In addition, this procedure indirectly yields information concerning the spins and parities of the levels in the Ne^{20} compound nucleus through which the reactions proceed.

The energy levels of O^{16} which are reached by the alpha particles from the reaction $F^{19}(p\,\alpha)O^{16*}$ have been known for some time.[1] The purpose in reëxaming the reaction was to determine if there was an energy level in the O^{16} nucleus in the excitation energy range 7-9 Mev, with a spin and parity assignment 2^-. The alpha particle model of the O^{16} nucleus[2,3] (four alpha particles at the vertices of a regular tetrahedron) indicated that there should be a more or less closely spaced doublet of levels, one level with spin and parity 2^+, the other 2^-. A 2^+ level had already been observed[4] at an excitation energy of 6.91 Mev[1], while no 2^- level had been reported. However, none of the experiments had been done with high enough resolution to resolve a very narrow doublet, nor had the region just above 7 Mev been carefully covered. Therefore it was felt worthwhile to use the high resolution equipment available in an attempt to see if the 2^+ level could be resolved into a closely spaced doublet. Since the actual separation of the doublet could not be estimated

accurately, the region of excitation just above 7 Mev was searched for a possible 2^- level (the region of lower excitation energy having been covered by Chao et al.[1]), and the 2^+ level itself studied to make certain that the 2^- level was not degenerate with it or too nearly so to be resolved in the energy measurements. The method of doing this was to observe the angular distributions of the alpha particles from the various resonance levels in Ne^{20} to the 2^+ level in O^{16}. Since these distributions depend upon the spin and parity values of the initial and final states (in addition to the orbital momenta of the incident and emitted particles) it was expected that a 2^- state degenerate with the 2^+ might be revealed by deviations from the angular distribution expected for a pure 2^+ level. In so doing additional information was obtained concerning the spins and parities of the Ne^{20} resonance levels, some of which had been known previously only from the simultaneous angular distribution measurements of the three gamma-rays from the 3^-, 2^+, and 1^- O^{16} levels to the ground state.[5] An energy level diagram showing the resonances concerned and the O^{16} final states, with their energies, spins and parities included, are shown in figure 1.

Another useful method of determining energy levels, which was used in the study of F^{19}, is to observe the inelastic scattering. In the case of the $F^{19}(p\ p')F^{19*}$ reaction, the incident proton is captured by the F^{19} nucleus, forming Ne^{20} in an excited state. The Ne^{20} nucleus then decays to a proton and a F^{19} nucleus in either its ground state or an excited state. In the former case one has elastic scattering, in the latter inelastic scattering. The difference in energy between protons scattered elastically and inelastically at a given

angle is due to the energy of excitation given to the residual F^{19} nucleus, and therefore to each inelastic proton group observed corresponds an excited state of F^{19}. In this way Cowie et al.[6] and Bender et al.[7] determined a number of levels in F^{19}. However, neither group reported protons corresponding to excited levels in F^{19} at 113 and 192 kev. These levels were reported by Mileikowsky and Whaling[8], who found two groups of alpha particles in addition to the ground state group while studying the reaction $Ne^{21}(d\,\alpha)F^{19}$, which corresponded to the above two excited levels. The same two levels were also reported by Day[9], who observed the gamma-rays from the reaction $F^{19}(nn',\gamma)F^{19}$. Therefore an experiment was started to see if the inelastic proton groups corresponding to the two levels could be observed and their energies determined. In addition, angular distributions were attempted in order to determine the spins and parities of the levels since it is of interest to compare this information with the shell model predictions of the F^{19} nucleus.

II THEORY OF THE EXPERIMENTS

1. The Alpha Particle Model of the O^{16} Nucleus.

The alpha particle model, which has been applied with some success to the O^{16} nucleus in the low energy region, has been discussed by Dennison[3] and others.[2] A brief summary of Dennison's theory will be given here. The O^{16} nucleus is thought of as a close-packed grouping of four alpha particles whose equilibrium configuration is that of a regular tetrahedron. The energy of the rotating, vibrating tetrahedral model is written as

$$W = \frac{(j^2+j)\hbar^2}{2A} + \hbar\omega_1\left(m_1+\tfrac{1}{2}\right) + \hbar\omega_2\left(m_2+1\right) + \hbar\omega_3\left(m_3+\tfrac{3}{2}\right) + I_{m_3 j} \pm \epsilon_i$$

where

A is the moment of inertia

ω_1, ω_2, ω_3 are three normal frequencies expressed in circular units, where ω_1 corresponds to an isotropic dilation of the nucleus, ω_2 corresponds to the motion in which the alpha particles are paired into two dumbells twisting with respect to each other, and ω_3 is the motion in which one dumbell lengthens while the other shortens, and vice-versa.

$I_{n_{3j}}$ represents an interaction between vibration and rotation which arises from the fact that the motion associated with the frequency ω_3 possesses an internal angular momentum $\xi\hbar$.

$\pm \epsilon_i$ denotes a contribution to the energy arising from the tunneling process by which a tetrahedron expressed in a right-hand coordinate system passes over into a tetrahedron in a left-hand system.

The states whose wave functions are invariant under an interchange of any two alpha particles (Bose-Einstein statistics) and which correspond to low rotational and vibrational quantum numbers are given in the following table.

n_1	n_2	n_3	j	P	W (theoretical)	W(observed) Mev
0	0	0	0	+	0	0
0	0	0	3	-	$6\hbar^2/A$	6.13
0	0	0	4	+	$10\hbar^2/A$	----
1	0	0	0	+	$\hbar\omega_1$	6.05
0	1	0	2	+	$3\hbar^2/A + \hbar\omega_2$	6.91
0	1	0	2	-	$3\hbar^2/A + \hbar\omega_2 + 2\epsilon_0$	----
0	0	1	1	-	$\hbar^2/A + \hbar\omega_3 + 9\hbar^2/8A + \epsilon_0 - \epsilon_1$	7.12

In this table the first four columns are the quantum numbers, the fifth column is the parity, and the sixth and seventh columns the calculated and observed energies of the levels. The term $9\hbar^2/8A$ in the sixth column represents the interaction energy, which for this state is $-(j+1)\xi\hbar^2/A + \xi^2\hbar^2/2A$; $\xi = -\frac{1}{2}$ when $n_3 = 1$.

The ω's may be found by the usual methods of normal coordinates. There are six internal coordinates; these may be chosen as the six displacements $q_1 \ldots q_6$ along the edges of the tetrahedron, where q_1, q_2; q_3, q_4; and q_5, q_6 represent displacements along opposite edges. The potential energy is a function of the q's and may be developed in a power series. Retaining no powers beyond the second, one gets:

$$V = \tfrac{1}{2}\Big[a(q_1^2 + q_2^2 + q_3^2 + q_4^2 + q_5^2 + q_6^2) + 2b(q_1q_3 + q_1q_4 + q_1q_5 + q_1q_6 + q_2q_3 + q_2q_4 + q_2q_5 + q_2q_6 + q_3q_5 + q_3q_6 + q_4q_5 + q_4q_6) + 2c(q_1q_2 + q_3q_4 + q_5q_6)\Big]$$

The three frequencies as a function of the constants a, b, and c together with M, the mass of an alpha particle, are:

$$M\omega_1^2 = 4a + 16b + 4c \quad ; \quad M\omega_2^2 = a - 2b + c \quad ; \quad M\omega_3^2 = 2a - 2c$$

The nature of nuclear forces indicates $a >> b$, $a >> c$; all other solutions are rejected as physically unlikely. The ϵ_i are estimated by Dennison from the theory of the two minima problem to be $\epsilon_1 = 25\epsilon_0$ and $2\epsilon_0/\hbar\omega_3 = 3 \times 10^{-3}$; the value of ϵ_0 may be underestimated, however.

The constants may be evaluated by a comparison with the observed energy levels. This has already been done by Inglis[10] and the following is essentially a summary of his calculations. First the moment of inertia parameter is determined by putting $6\hbar^2/A = 6.13$ Mev. (This

gives a value of 2.5×10^{-13} cm. for the nuclear radius of O^{16}, which is low compared with $R_o A^{1/3} \approx 1.2 \times 16^{1/3} \times 10^{-13} \approx 3 \times 10^{-13}$ cm., even with the recent low value for R_o.) Next, the first vibration frequency is obtained from $\hbar\omega_1 = 6.05$ Mev, and the second vibration frequency from $\hbar\omega_2 = 6.91$ Mev $- 3\hbar^2/A = 3.85$ Mev. Neglecting ϵ_0, one gets $\hbar\omega_3 - \epsilon_1 = 7.12 - 17/8(1.022)$. Using Dennison's estimate from the theory of the two minima problem, one has $\epsilon_1 \approx 0.04\ \hbar\omega_3$, or, from the above, $0.96\ \hbar\omega_3 = 4.95$ Mev. Then $\hbar\omega_3 = 5.16$ Mev, $\epsilon_1 \approx 206$ kev, and $\epsilon_0 \approx 8$ kev. (Solving for a, b, and c gives $\sim 66{:}{-4.7}{:}1$ for the ratios a:b:c, and b and c are much smaller than a as required.) This would predict a separation of about 16 kev ($2\epsilon_0$) for the doublet, which is quite capable of being resolved by the spectrometer used. However, it must be emphasized that this value depends upon Dennison's estimate of ϵ_0, which may be low; ϵ_0 could conceivably be of the order of several Mev. Therefore a complete range of energies, from zero (complete degeneration) to about 2 Mev separation was examined for a 2^- level (including degeneration with the 1^- level).

2. Angular Distributions.

a. The General Particle Reaction X(ab)Y.

Consider first a reaction in which the incident particle a is captured by the target nucleus X, forming a compound nucleus C, which then decays into a particle b and residual nucleus Y. In the formation and subsequent decay of the compound nucleus, the differential cross section for particle emission goes as the product of two matrix elements, one for the formation of the compound nucleus and one for

its decay. The matrix elements are then resolved into an unknown factor which depends upon the nuclear properties of the process, and a transformation coefficient for the combination of angular momenta, which is known.(11)

Let the incoming particle define a z-axis. If the spin of the particle is combined with the spin of the target nucleus to give channel spin s with projection on the z-axis s_z, this channel spin must be combined with the orbital angular momentum ℓ of the particle with projection zero on the z-axis to give the spin J with its projection M of the compound nucleus. Let the combined spins of the emitted particle and residual nucleus be s' with projection s_z', and the relative orbital angular momentum of the two particles be ℓ' with projection m'. Then the function describing the angular distribution of the outgoing particles relative to the incoming particle beam is:

$$W(\theta)=\sum_{s,s_z}\sum_{s',s_z'}\left|\sum_{\ell}(2\ell+1)^{1/2}f_i(\ell)\langle s,s_z;\ell,0|J,M\rangle\right|^2\cdot\left|\sum_{\ell'}f_e(\ell')\langle J,M|s',s_z';\ell',m'\rangle Y_{\ell'}^{m'}(\theta,0)\right|^2 \quad (1)$$

where $f_i(\ell)$ and $f_e(\ell')$ are complex factors describing the probability amplitudes associated with the different orbital momenta, and $Y_{\ell'}^{m'}$ is a spherical harmonic. The factors in the brackets $\langle\ \rangle$ are Clebsch-Gordan coefficients, useful tables of which are compiled in a thesis by Dr. A. A. Kraus.(12) The sums are taken over the various possible values of the channel spins and their projections, together with the allowed values of the orbital momenta. The terms belonging to different values of the orbital momenta must be added coherently, while

the various channel spins add incoherently. However, for more than one channel spin an arbitrary coefficient is assigned to each, which gives the probability of the reaction proceeding by that channel spin. These probabilities are not calculable in general, and introduce an ambiguity into the distribution. It is to be noted that there is no sum over levels of the compound nucleus, which assumes that only one level of the compound nucleus contributes to the reaction. This assumption gave agreement with the observed results in all but one case. A distribution will be given later which considers two or more levels of the compound nucleus contributing to a reaction.

b. The Reaction $F^{19}(p\,\alpha)O^{16*}$

In this reaction the incident proton is captured by the F^{19} nucleus to form Ne^{20} in an excited state. The Ne^{20} compound nucleus then decays into an alpha particle and an O^{16} nucleus, which may be in either its ground state or an excited state. Five groups of alpha particles have been observed from the reaction.[1] Three groups go to gamma-ray emitting levels at 6.13, 6.91, and 7.12 Mev. For convenience, the alpha particle groups to these levels have been labelled α_1, α_2, and α_3[1] in order of decreasing alpha particle energy. Seed and French have made the assignments 3^-, 2^+, and 1^- [4] to these levels, in order of increasing excitation energy, on the basis of the α-γ angular correlations. Another alpha particle group (denoted by α_π) goes to a pair emitting level at 6.05 Mev which has spin and parity 0^+. The usual selection rule on gamma-rays (no $0 \longrightarrow 0$ transition) prevents this mode of decay to the ground state, which has spin and parity 0^+ also. The alpha particles to the ground state are denoted

by α_0 and are the maximum energy alpha particles from this reaction. A complete discussion of these groups, together with excitation curves and cross sections has been given by Chao et al.[1] The resonances which yield the α_γ groups seem to be distinct from those yielding α_π's and α_0's (both go to 0^+ levels). This is usually assumed to be due to the need to conserve angular momentum and parity. If the Ne^{20} levels going to the gamma-ray emitting states in O^{16} are assumed to have either even spin values with odd parity, or odd spin with even parity, then they will not decay to the 0^+ levels. Although this assumption gives good agreement with the experimental data, it does not prove conclusively that there is not another selection rule in operation. If one makes this assumption, then those Ne^{20} levels which go to gamma-ray emitting levels in O^{16} can be formed only by channel spin 1. (In general, both channel spin 0 and 1 are possible, since the proton and the F^{19} nucleus each have spin $\frac{1}{2}$). For if one uses channel spin 0, then the orbital angular momentum of the proton gives the spin of the compound nucleus and also its parity (since both the proton and F^{19} have even parity). But an odd orbital momentum value then gives an odd parity state, and an even value an even parity state, and thus channel spin 0 must be ruled out. Then we can remove the sum over s in formula (1). A second simplification which may be made is that the alpha particle has spin 0, and therefore the outgoing channel spin s' is just the spin of the residual O^{16} nucleus, which is denoted by J', with projection M'. Then formula (1) reduces to

$$W(\theta)=\sum_{s_z,M'}\left|\sum_{\ell}(2\ell+1)^{1/2}f_i(\ell)\langle s,s_z;\ell,0|J,M\rangle\right|^2\cdot\left|\sum_{\ell'}f_e(\ell')\langle J,M|J',M';\ell',m'\rangle Y_{\ell'}^{m'}(\theta,0)\right|^2 \qquad (2)$$

Thus there are no arbitrary coefficients due to channel spin, and the resultant distributions are quite unambiguous. Frequently only the lowest possible values of ℓ and ℓ' need be considered for particle energies well below their respective barrier heights, but the experimental results indicated that the higher values of orbital momenta could make measurable contributions.

Perhaps a little simpler formula to use is that given by Blatt and Biedenharm[13], using their Z coefficients which are tabulated in an Oak Ridge National Laboratory Report.[14] The Z coefficients are combinations of the W coefficients of Racah.[15] Angular distributions written in terms of Z coefficients involve less summations in that their use effects the summations over the magnetic quantum numbers. When written in terms of Z coefficients formula (2) becomes:

$$W(\theta) = \sum_{L} \sum_{\ell_1} \sum_{\ell_2} \sum_{\ell_1'} \sum_{\ell_2'} f_i(\ell_1) f_i(\ell_2) Z(\ell_1 J \ell_2 J; sL) f_e(\ell_1') f_e(\ell_2') Z(\ell_1' J \ell_2' J; J' L) P_L(\cos\theta) \tag{3}$$

where $L = 0,2,4,\ldots \min.(2\ell, 2\ell', 2J)$ and $P_L(\cos\theta)$ is the Legendre polynomial. If one considers only the lowest values of orbital momenta, formula (3) reduces to the extremely simple form:

$$W(\theta) = \sum_{L} Z(\ell J \ell J; sL) Z(\ell' J \ell' J; J' L) P_L(\cos\theta) \tag{4}$$

The pertinent distributions are listed in Appendix I. A distribution is labelled by the four numbers $(\ell, J; \ell', J')$ where the nomenclature is the same as before. For 2 possible channel spins, the distribution due to channel spin 0 was multiplied by 1 and that due to channel spin 1 by C. Where more than the lowest orbital momenta are considered, the higher values are also listed in brackets. Thus

(1(3),2;1(3),2) would give the distribution for p- and f-wave protons forming a 2^- level in Ne^{20}, which then goes to the 2^+ level in O^{16} with the emission of p- and f-wave alpha particles. Those distributions which consider higher values of the orbital momenta have been taken from the tables of Seed and French.[4] Their treatment of the orbital momenta is as follows. Consider the Ne^{20} compound nucleus being formed by protons of orbital momenta ℓ and $\ell + 2$, and alpha particles emitted with relative orbital momenta ℓ' and $\ell' + 2$. Then put

$$f_i(\ell + 2)/f_i(\ell) = Ae^{i\alpha} \quad \text{and} \quad f_e(\ell' + 2)/f_e(\ell') = Be^{i\beta}$$

where α and β represent the phase differences between interfering states of the system and A and B their relative amplitudes. The phase shift, apart from an uncertainty of π, associated with an orbital momentum ℓ in a Coulomb field is given by

$$\delta_\ell = -\tan^{-1}\frac{F_\ell}{G_\ell} - \eta \log 2kR + \sigma_\ell - \tfrac{1}{2}\ell\pi$$

where F_ℓ, G_ℓ are the regular and irregular solutions of the Coulomb wave equation; $\eta = z_1 z_2 e^2/\hbar v$; $k = \mu v/\hbar$, μ being the reduced mass of the system; R is the nuclear radius and $\sigma_\ell = \arg(\ell + 1 + i\eta)$. In this experiment the proton and alpha particle energies were well below the respective barrier heights so that $F_\ell << G_\ell$ and the phase difference between two waves of orbital momenta ℓ and $\ell + 2$ becomes

$$\delta_{\ell,\ell+2} = \sigma_{\ell+2} - \sigma_\ell - \pi = \tan^{-1}\frac{\eta}{\ell+2} + \tan^{-1}\frac{\eta}{\ell+1} - \pi$$

c. Interfering Levels of the Compound Nucleus.

When two or more levels of the compound nucleus contribute significantly to a reaction a summation must be made over the levels involved, with arbitrary amplitudes and phases for the contribution

from each level. In general these parameters are quite rapidly varying functions of the bombarding energy. Thus a small change in bombarding energy can cause a large variation in the measured angular distribution. The angular distribution may be written (for the lowest orbital momenta values)

$$W(\theta)=\sum_{S,S_z,M'}\left|\sum_{J_i}A_i e^{i\alpha_i}\langle S,S_z;\ell_i,0|J_i,M_i\rangle\langle J_i,M_i|J_i',M';\ell_i',m_i'\rangle Y_{\ell_i'}^{m_i'}(\theta,0)\right|^2 \quad (5)$$

where A_i and α_i are the amplitude and phase associated with particles from the i th level. The Coulomb phase shift, which may be calculated, can be written separately from the α_i if desired. The dependence of the arbitrary amplitudes upon bombarding energy may be specified in more detail by use of the dispersion formula of Breit and Wigner (see for example Chao[11]); however, an arbitrary factor always remains and this explicitness adds little in trying to fit the experimental data. What is of interest is to see if the observed distribution can be fitted by considering interference, what the spin and parity of the interfering level (or levels must be), how much relative intensity from the interfering level is necessary, and if sufficient data is available, to determine if the theoretical distribution varies in the manner observed as the bombarding energy is changed. In general, interference effects can modify angular distributions considerably, and a complete analysis is difficult and requires extensive data.

d. The Reaction $F^{19}(p\,p')F^{19*}$

For this reaction formula (1) gives the angular distribution of the inelastic protons. Again only channel spin one was considered in

the formation of the compound nucleus, as none of the resonances used was a long-range alpha particle or pair resonance. However, since in this case the outgoing particle is a proton with spin $\frac{1}{2}$, there are in general two values of the outgoing channel spin. This introduces an ambiguity into the distributions as mentioned before. Take the probability associated with channel spin s' to be $A_{s'}$. Now the distribution for the inelastic protons may be written:

$$W(\theta)=\sum_{S_z}\sum_{S',S'_z}\left|\langle S, S_z; \ell, 0 | J, M\rangle\right|\cdot\left|A_{s'}^{1/2}\langle J, M | s', S'_z; \ell', m'\rangle\, Y_{\ell'}^{m'}(\theta, 0)\right|^2 \qquad (6)$$

The pertinent distributions are listed in Appendix II. For each value of spin for the final state in F^{19} are two possible outgoing channel spins. Since the ratio of the two values of the channel spin is what determines the resulting angular distribution, the distribution due to the lower channel spin has been multiplied by 1, and that due to the higher channel spin by C. C then gives the ratio of the two competing channel spins. The distributions associated with each channel spin are extreme distributions (i.e. the reaction proceeding entirely by either one channel spin or the other). The observed distribution may be any linear combination of these. Thus a unique distribution is not predicted, but rather a continuous range of distributions.

III. APPARATUS AND EXPERIMENTAL PROCEDURE

1. High Resolution Study of the α_2 and α_3 Groups at 874 kev.

The 2 Mv. electrostatic generator of this laboratory was used to accelerate the protons, which were then passed through an 80 degree

electrostatic analyzer which rendered them homogeneous to ± 0.05 percent. The outgoing reaction products were analyzed by a 180 degree double focussing magnetic spectrometer of $10\frac{1}{2}$" radius. A regulator on the magnet kept the current constant to ± 0.02 percent. The detection was done either with photographic plates or scintillation counter (a zinc sulfide screen followed by a 931A photomultiplier tube).

In all phases of the work good targets were of prime importance. This was particularly true in the case of the high resolution study of the α_2 and α_3 groups; thin targets were essential. The targets used in this portion of the work were of sodium fluoride evaporated in vacuum onto a thin aluminum foil (0.2 mg./cm.^{2}) which was supported on an aluminum frame. The sodium fluoride was evaporated onto the aluminum foil from a small tantalum boat placed in the bottom of the target chamber, in order that the targets need not be exposed to air. Target thicknesses were determined by using a Geiger-Müller counter coincidence arrangement[16] at 90 degrees to the beam to run the excitation curve of the gamma-rays over the resonance (874 kev), and then using the relation $\xi = (\Gamma'^2 - \Gamma^2)^{\frac{1}{2}}$ where Γ' is the observed half-value width and Γ the true half-value width of the resonance, as given by Bonner and Evans.[17] All quantities are expressed in energy units.

The detection in this part of the experiment was done with photographic plates in order to get a little higher resolution. In order to get high resolution with the counter a narrow slit width must be used. This gives a very low yield and means taking lengthy runs at many points to establish the total yield, with target deterioration and the build-up of contamination on the target surface due

to the bombardment becoming important effects. With the plates, however, the whole profile is obtained in only one run, and in addition, a good deal of the background on either side of the peak. This means that a relatively large range in excitation energy is covered by the plate in one run, which would take many runs with the counter. Effects such as change in amount of bombardment due to change in integrator firing voltage and change in effective target thickness due to motion of the beam spot on the target are eliminated by this procedure. Ilford C_2 plates were used, 1" x 3", with a 100 micron emulsion thickness. A camera was built (fig. 2) which placed the long axis of the plate in the exit focal plane of the spectrometer; the short axis made an angle of 30 degrees with the incident alpha particles. The plate could be withdrawn from this position and exit slits moved into the focal plane without breaking the vacuum. Just to the rear of the focal plane was the zinc sulfide screen followed by a photomultiplier tube. The method used in taking a plate was as follows. After a good target was obtained and the bombarding energy set to give the maximum gamma-ray yield, a profile of the alpha particle group being studied was run with the scintillation counter. (A profile is a yield vs. $H\rho$ curve.) Then the magnet current was set to give the peak of the alpha particle group, the plate put in place, and a run made. Continuous monitoring of the gamma-ray yield served as a check upon target deterioration. The total amount of bombardment was determined by a current integrator. When the desired amount of bombardment was completed, the plate was removed and the counter used to run the alpha particle profile

again. A shifting of the peak of the group towards lower energy would have given an indication that surface contamination was building up on the target due to the bombardment, but this effect was found to be negligible. If present to a large extent, such an effect could smear out a closely spaced doublet into a single peak. A cold trap between the target and oil diffusion pump trapped out most of the oil vapors.

Once the plate was exposed, it was developed and the alpha particle tracks counted. The microscope used for this purpose was fitted with a mechanical stage driven by two micrometer screws at right angles, which were capable of reproducing any setting to $\pm$ 3 microns. A 25x objective and 8x eyepiece with counting reticle were used. At this magnification the reticle covered an area approximately $\frac{1}{2}$ mm. x 1/3 mm. on the plate. The position of the tracks measured parallel to the long axis of the plate was a measure of the energy of the particle. Thus all tracks in a band 1/3 mm. wide parallel to the short edge of the plate were counted as being due to particles with the same energy range (between say some value E and E + δE). Then the reticle was moved 1/3 mm. and all tracks in the next band counted. In this way the entire plate was scanned. The length of the band in which an appreciable number of tracks were found was about 6 mm., since the double focussing property of the spectrometer tended to keep the particles in a narrow strip. The change in energy per unit length along the photographic plate can be calculated from the formula

$$R = P/\delta P = 2E/\delta E = 3.6r_o/\delta r$$

where R is the resolution of the spectrometer, P and E the momentum

and energy of a particle in the equilibrium orbit (which may be calculated from the fluxmeter setting and calibration constant of the spectrometer), r_o is the radius of the equilibrium orbit (10.5"), and δr is the distance in the focal plane through which a beam of particles of energy $E + \delta E$ is displaced from one of energy E. For the spectrometer used $E = E\,\delta r/480$ for δr in millimeters. In this way the width of the peak at half maximum in energy units was determined from the measured width in millimeters, and was used in setting an approximate upper limit on the separation of any doublet which might exist, as only one group was observed.

2. Angular Distributions of the Reaction $F^{19}(p\,\alpha)O^{16*}$

In measuring the angular distributions of the alpha particles from the reaction, good targets were again essential, but here the thickness was not so critical and was in general on the order of 5 kev thick for protons of the particular bombarding energy used. Targets were made exactly as above, but the target material was principally zinc fluoride. The gamma-ray counter was used to measure the target thickness, after which the bombarding energy was set to give the maximum gamma-ray yield. Periodically during runs the gamma-ray excitation curve was run to see whether the resonance peak had shifted, indicating the build-up of surface contaminations on the target. (Since the beam is reduced in energy by the time it has passed through the surface layer, the peak comes at higher bombarding energy). Whenever such a shift was observed, the bombarding energy was increased to give the peak gamma-ray yield as before.

Instead of using a current integrator to determine the amount of bombardment, a fixed number of gamma-ray counts were run at each point

taken, with the counter at 90 degrees to the proton beam. This method corrects for any change in target thickness due to the motion of the beam spot on the target from run to run.

In measuring angular distributions the target was held fixed at either of the two angles $+45^{\circ}$ or -135° with the incident beam. (The direction of motion of the protons, and of the outwardly drawn normal from the fluorided side of the target being taken as positive). The target was set at -135 degrees for angles of observation greater than 90 degrees, and at +45 degrees for angles less than 90 degrees. In this way the target thickness was held constant for all angles of observation, and no correction had to be made for change in effective target thickness, as would have been the case if the target was set so that at each angle of observation the normal to the target bisected the angle between the beam and the emitted alpha particles, which is another way of setting the target angle. With the target at +45 degrees (transmission) the alpha particles from the reaction passed through the target backing foil before entering the spectrometer while with the target at -135 degrees (reflection) they passed back out through the target material again before entering the spectrometer. The foil thickness (0.2 mg./cm.^{2}) was such as to decrease the alpha particle energy by about 200 kev. This had the advantage that particles emitted in the forward direction, which are more energetic than those at back angles, were slowed by the target backing foil. Since the limit of the spectrometer was 2 Mev alpha particles, some slowing by foils was necessary. (For this reason the only resonance at which the α_1 group was studied was at 874 kev, and there only at

back angles. It would have required too many foils to observe this group elsewhere, with the result that there would have been an undesirable amount of straggling.) In addition to the target backing foil, through which all of the alpha particles passed at forward angles, a foil holder was inserted between the target and the spectrometer, and as close to the target as possible. Up to two additional foils were used with this holder at the higher energy resonances and at forward angles. For each number of foils used a correction factor for loss of particles in the foils was determined experimentally by comparing yields which could be obtained both with and without foils.

The angles of observation were chosen so as to divide the interval of $\cos^2\theta_{cm}$ from zero to one into eight equal parts. All distributions were plotted vs. $\cos^2\theta_{cm}$ for ease in comparison with the theoretical distributions. When plotted in this way all of the distributions obtained were fitted reasonably well with either straight lines or parabolas.

The method of obtaining an angular distribution was to run the desired alpha particle group profile at each angle, with the proton energy set to give the maximum gamma-ray yield. The total number of counts at each angle was obtained by integrating graphically the area under each profile according to the thin target formula[18]

$$Y \sim \int \frac{N(I)}{I}\, dI$$

where I is the fluxmeter setting (and is inversely proportional to the magnetic field), N(I) is the number of alpha particle counts obtained at the fluxmeter setting I, and dI is the interval used in integrating

the curve. It is sufficiently accurate, since the peaks are quite narrow, to replace the value of I in the denominator of the above expression by an average value $\bar{I}$; namely, that value which it has at the peak of the profile. Then

$$Y \sim 1/\bar{I} \int N(I)dI = A/\bar{I}$$

where A is the area under the curve. In order to compare the yields in the center of mass system, this quantity must be transformed to the center of mass system. The solid angle may be transformed by the relation

$$\frac{d\Omega_{cm}}{d\Omega_L} = \frac{(1 + 2\alpha\cos\theta_{cm} + \alpha^2)^{3/2}}{1 + \alpha\cos\theta_{cm}} \approx 1 + 2\alpha\cos\theta_{cm}, \quad \alpha << 1$$

where

$$\alpha = \left[\frac{M_1M_2E_1}{(M_1 + M_0)M_3Q + M_0M_3E_1}\right]^{1/2}$$

Here M_0 is the mass of the target nucleus, M_1 the mass of the incident nucleus, M_2 the mass of the observed particle, M_3 the mass of the residual nucleus, E_1 the proton energy, and Q is the energy release $(M_0 + M_1 - M_2 - M_3)c^2$. The angle of emission in the center of mass system θ_{cm} is related to that in the laboratory system θ_L by the relation

$$\text{ctn}\,\theta_L = \text{ctn}\,\theta_{cm} + \alpha\,\text{csc}\,\theta_{cm}$$

In addition to transforming to the center of mass system a small correction was applied to each yield for the number of uncounted singly charged He^+ ions according to Thomas et al.[19] Then the corrected yield in the center of mass system is given by

$$Y_{cm} = Y_{Lab} \cdot \frac{d\Omega_L}{d\Omega_{cm}} \cdot (1 + He^+/He^{++})$$

The total corrected yield at each angle was then normalized to unity at 90 degrees, and plotted vs. $\cos^2\theta_{cm}$, forward and back angles being

plotted separately to display the fore and aft symmetry observed.

3. The $F^{19}(p\ p')F^{19*}$ Reaction.

In studying the inelastic protons corresponding to the first two known excited levels of F^{19}, the target materials used were principally aluminum fluoride (Al_2F_6) and lithium fluoride (LiF). Here different target backing materials were also used. Since the Q-values for these reactions (equal to the negative of the excitation energy of the level) are so small, the inelastic groups fell quite close to the elastic group from F^{19}. This meant that protons scattered with slightly less energy than those scattered elastically from F^{19} would fall in the region of interest. Thus the elastic protons from carbon and oxygen (which are always present in the pump oil vapor), from the target backing material, and from the other element which made up the fluorine compound were always present near or in the region of interest. In addition, when the target backing used was thin (which it was in the case of the aluminum backing) the same oxygen and carbon contamination built up on the rear surface of the target backing foil and gave two additional elastic peaks. The main experimental problem was to observe the inelastic groups away from the elastic groups, and at a sufficient distance that one could make a reasonable estimate of the background, and hence of the area under the profile of the inelastic group studied. Two different target backings were used for this purpose. In some cases a thick layer of lithium was put down on a copper backing (the lithium necessarily being thick enough to move the protons scattered elastically from the copper well behind the inelastic peaks), and then a thin target of aluminum or lithium fluoride put down.

For this purpose a new base was installed in the bottom of the target chamber which carried three water cooled electrodes instead of the usual two, in order that either of two tantalum boats might be heated independently of the other. In an initial attempt a single furnace was used. After filling the bottom of the furnace with aluminum fluoride, a piece of lithium was wedged in on top. Since lithium comes off at the lower temperature, the furnace was heated gradually until the lithium started to evaporate and then the target put in the evaporating position and a thick layer of lithium put down. Then the target was removed and the furnace heated slightly more for a short period to drive off any lithium that might be left. Finally the furnace was heated still more until the aluminum fluoride began to evaporate and then a thin layer of this laid down. The difficulty with the procedure was that the lithium could never be completely driven off, and continued to be put down with the aluminum fluoride, thus putting down the aluminum fluoride in a thicker but less dense layer. In addition, an undesirable amount of contamination seemed to accompany this method. The two furnace method gave very satisfactory targets, however. Since the lithium is quite light (mass number 7), the protons scattered elastically from it are far back of the desired groups at angles greater than 90 degrees, and it was possible to observe the inelastic groups forward of the lithium peak. Since the target backing was thick there was no problem of peaks from contamination on the back of it.

In other cases a thin aluminum foil was used as target backing material (0.2 mg./cm.^{2}). Aluminum, being a heavier element (mass number 27), had its elastically scattered protons well forward of the two groups.

However, the foil had some thickness, and gave scattered protons with a finite range of energy, those protons scattered from the rear surface of the foil having the least energy. In addition, there were always two peaks each due to protons scattered elastically from oxygen and carbon; one due to the layer on the target surface and one due to the layer on the back of the foil. Thus there were a very large number of undesired peaks, from which the inelastic peaks not only had to be identified, but also moved clear enough so that the total number of counts due to the inelastic scattering alone could be estimated with reliability. Due to the difficulties involved only very scanty information was obtained on the angular distributions, although it was always possible to get each group clearly resolved at one angle at each resonance used so that the energy of the group and thus the excitation of the level could be calculated.

IV. DISCUSSION OF RESULTS

1. Existence of the Predicted 2^- Level in O^{16}.

Good profiles were obtained with the photographic plates at a bombarding energy of 874 kev of the α_2 group at θ_{lab} = 90, 137.8 and 157.7 degrees, and of α_3 at θ_{lab} = 157.7 degrees. These curves are displayed in figs. 3-6. There is no evidence of doublet structure in any of the curves, all of the peaks being quite symmetrical. In addition, in the best case for each group, the width at half maximum of the peak is less than 6 kev. This leads to the conclusion that if the 2^+ level is actually a doublet, the separation is probably less than 3 kev, or more than 100 kev (since this was the energy range covered by the photographic plate).

In searching for a 2^- level separated by more than 100 kev from the known level, the region of excitation energy higher than the 1^- level at 7.12 Mev was examined, the region of lower energy being covered by Chao et al.[1] The proton energy was set at 874 kev and shorter range alpha particles than the α_3 group looked for. In this way the excitation range in O^{16} from 7.12 to 9.1 Mev was covered without finding any new alpha particle groups. This is an indication that there are no levels in O^{16} in this region of excitation. The examination was not conclusive, however, in that there might be a selection rule preventing alphas going to an unknown level. (At least, if not completely forbidding the transition, making it so weak as to be unobserved in this experiment.) Thus levels in this region could conceivably show up in other reactions. (A level was reported at 8.6 Mev by Fulbright and Bush on the basis of the inelastic scattering of protons from O^{16}.)[20]

In order to determine if there was a 2^- level closer than 3 kev to the 2^+ level (or possibly the 1^- level), the angular distributions of the alpha particles to these levels were observed. Since the angular distributions depend upon the spin and parity values of the initial and final states (in addition to the orbital momenta of the protons and alpha particles), this method could reveal a 2^- level even if it were completely degenerate with either known level. With the bombarding energy at 874 kev, the α_2 group was observed at forward and back angles, and the angular distribution $1 - 0.65 \cos^2\theta$ obtained. (Fore and aft symmetry was observed; see fig. 9). The 874 kev resonance level had already been determined to be 2^- by Seed and French[4]; this is in

agreement with the assignments of Chao[5] and Sanders[21] on the basis of gamma-ray angular distributions, and with elastic scattering measurements made in this laboratory. If one looks in table I for the transition $Ne^{20}(2^-) \longrightarrow O^{16}(2^+)$, considering only the lowest values of ℓ and ℓ' ($\ell = 1, \ell' = 1$), the theoretical distribution is $1 - 7/9 \cos^2\theta$. The observed coefficient is lower than the predicted one by some 17 percent. Suppose that there were a 2^- level almost or completely degenerate with the 2^+ level. For a 2^- O^{16} level, the lowest permitted values of orbital momenta would be $\ell = 1, \ell' = 0$. Thus s-wave alpha particles would be possible, and their barrier penetration factor would be lower than for the p-wave alpha particles from the 2^+ level. If these barrier penetrabilities are calculated on the WKB approximation given by Bethe[22], one gets for the ratio P_1/P_0 (where P_ℓ is the barrier penetrability associated with orbital angular momentum ℓ) 0.45. Then, observing the distribution from a Ne^{20} 2- level to the two O^{16} levels with assignments 2^+ and 2^- simultaneously, one would expect the alpha particles to the 2^- level to be favored. The ratio of the intensity of alpha particles to the 2^- level to the intensity of those to the 2^+ level necessary to give the observed distribution may be calculated. Since the alpha particles to the 2^- level are s-wave their distribution will be isotropic. Then $I_{2^-} + I_{2^+} (1 - 0.78 \cos^2\theta) = (I_{2^-} + I_{2^+})(1 - 0.65 \cos^2\theta)$ where I is the intensity. This gives $I_{2^-}/I_{2^+} = 1/5$. Although this could be all the relative intensity to the 2^- level, since barrier factors alone do not determine the relative rates of the transitions, it seems rather small. However, the reduced value of the coefficient may be satisfactorily accounted for without the presence of a 2^- level by taking into account the other two orbital momenta values possible in this transition; namely,

$\ell = 3$ and $\ell' = 3$. First consider the a_3 angular distribution at the same resonance (fig. 10). Since only one value of ℓ' is allowed ($\ell' = 2$), this distribution is not a function of B or cos β. The absolute value of cos α was calculated to be 0.438. A is expected to be small, as it is the ratio of the amplitudes for penetrating the barrier of F^{19} by protons of 874 kev energy, with orbital momenta 3$\hbar$ and 1$\hbar$ respectively. Then if only terms to first order in A are retained, the theoretical distribution one gets from Appendix I is $W(x) = 1 + x + 2(2/3)^{\frac{1}{2}} A \cos\beta(1 - 9x + 10x^2)$, where $x = \cos^2\theta$. In figure 7 a plot of W(x) is made for several small values of A, and cos α both positive and negative. For all values of A the curve passes through the point (1,2). At any fixed value of x, equal changes in A for small A produce roughly equal changes in W(x). For A equal to zero, the curve is linear, and for values of A other than zero, the distribution is parabolic, bending above the A = 0 distribution for cos α negative and below it for cos α positive. The effect of the higher ℓ values is to add some curvature to the distribution. Thus this data gives the sign of cos α and a rough value of A (really an upper limit). Having obtained A and the sign of cos α in this manner, they may be used in the distribution to the 2^+ level from this same resonance, since they depend only upon which resonance in Ne^{20} is used. When this is done, the only arbitrary parameters in the a_2 angular distribution are B and the sign of cos β. When all terms of second order or higher (other than B^2) are neglected the distribution is linear. Thus a value of B and the sign of cos β may be determined from a least squares fit of the data. In this way A was determined to be 0.06 and

B 0.29. These values are reasonable in magnitude and agree fairly well with those Seed and French[4] obtained from the angular correlation measurements. ($A = 0.1 \pm 0.1$, $B = 0.35$). Thus the lowering of the coefficient is entirely consistent with the known levels. It is to be noted that the angular distribution of the α_3 group at this resonance, which is in satisfactory agreement with the above level assignments, would also be markedly altered by the presence of a 2^- level close to the 1^- level, and could easily have been detected.

2. Angular Distributions of the Reaction $F^{19}(p\,\alpha)O^{16*}$

The results of the angular distribution measurements are listed in the following table.

TABLE I.

Angular Distributions of the Reaction $F^{19}(p\,\alpha)O^{16*}$

Resonance (kev)	Alpha Group	A	B	$\cos\alpha^*$	$\cos\beta^*$	Measured Distribution
874	α_1	0.06	0.37	0.438	-0.242	$1 - 0.49x$
874	α_2	0.06	0.29	0.438	-0.250	$1 - 0.65x$
874	α_3	0.06		0.438		$1 + 0.61x + 0.39x^2$
935	α_3					1
1290	α_2					1
1290	α_3					$1 + x$
1355	α_2	0.14	0.43	0.595	-0.156	$1 - 0.63x$
1355	α_3	0.14		0.595		$1 - 0.19x + 1.19x^2$
1381	α_2					$1 - 0.43x$
1381	α_3					1

* The magnitudes of these phase shifts are calculated as given in the theory; the sign is determined experimentally.

After the α_2 and α_3 groups were observed at the 874 kev resonance to determine whether or not a 2^- level was degenerate with either the 2^+ or the 1^- level, the α_1 angular distribution was measured at this resonance. Since the energy of the alpha particles was so high the distribution was only measured at back angles, and it required three foils to get the alpha particles through the spectrometer. However, the α_1 group is the most intense of the three groups, and good statistics were obtained without an intolerable amount of straggling. The distribution agreed with the 2^- assignment to the Ne^{20} level and 3^- to the O^{16} level (the coefficient again being slightly lower than one would expect taking into account only the lowest ℓ values; this was again satisfactorily explained by considering the next two higher permitted values of the orbital momenta). This was the only resonance at which the α_1 group was observed, the α_1 groups from the higher energy resonances being too energetic to be feasibly slowed down by foils.

As a check on the theory, the angular distributions of the α_3 group at the 935 kev resonance was measured next. The 935 kev resonance level is a 1^+ state, and hence may be formed by s-wave protons. Thus the distribution should be mainly isotropic, with higher ℓ values modifying the distribution slightly. ℓ' has only the value 1, but ℓ may be either 0 or 2; A should be small and $|\cos \alpha| = 0.038$. Therefore the effect of the higher ℓ values is negligible, and the distribution measured was indeed isotropic. (fig. 11) The α_2 group was so weak at this resonance that no attempt was made to determine its distribution.

With this satisfactory check, the distributions were next measured at the 1355 kev resonance level. The only information as to

the spin and parity of the level came from the data of Day et al.[23] on the simultaneous angular distribution of the three gamma-rays as analyzed by Chao.[5] Chao found that satisfactory agreement could be had by assuming the level to be either 2^- or 3^+. The alpha particle distributions, which were quite similar to those at the 874 kev resonance level, led to a 2^- assignment for the level. This assignment has recently been checked by the elastic scattering of protons from F^{19} done in this laboratory. The assumption of p- and f-wave protons forming a 2^- Ne^{20} level, which goes by p- and f-wave alpha particles to the O^{16} 2^+ level, and by d-wave alpha particles to the O^{16} 1^- level gave a very satisfactory fit to the data, as may be seen in figs. 12 and 13. The distributions are listed in table I.

The yields of the α_2 and α_3 groups at the 1290 kev resonance were quite small and made accurate analysis impossible without further painstaking experimentation. A glance at the yield curves of Chao et al.[1] for the gamma-ray yield at this resonance shows that one might expect the background yield to be of the same order of magnitude as the alpha particle intensity from the resonance itself. The angular distributions are those obtained at resonance, with the background yield included. Only back angles were used as foils would have reduced the already small counting rate. The distributions obtained are not inconsistent with the assignment of 3^+ made to this level by Chao[5], assuming a constant background yield at each point of relatively large magnitude with no interference. However, no positive assertion as to the assignment can be made on the basis of this data. The anomaly in the elastic scattering was also so weak that no analysis was attempted.

The 1381 kev resonance level had been previously studied by Day et al.[23], who measured the combined angular distribution of the three gamma-rays from the gamma emitting levels in O^{16} (those from the 1^-, 2^+, and 3^- levels to the ground state of O^{16}, of energies 7.12, 6.91, and 6.14 Mev respectively.) The work was done with Geiger-Müller counters with no possibility of resolving the three gamma-rays. At all bombarding energies they observed distributions which could be fitted with curves of the form $1 + a \cos^2\theta$. However, as the bombarding energy was varied across the resonance, the coefficient was found to vary linearly from -0.2 to 0.1, with the value -0.073 at the resonance. This behavior suggests the possibility of interference, although it could result merely from the change in the relative amounts of the three gamma-rays as the bombarding energy is changed. On the basis of the smallness of the coefficient at resonance, and of the ratio of gamma-ray intensity at 90 degrees to alpha particle intensity at 137.8 degrees[1], Chao[5] made the assignment 1^+ to this level.

The distributions observed at the resonance for the alpha particle groups were isotropic for the α_3 group and $1 - 0.43 \cos^2\theta$ for the α_2 group. It was found impossible to fit this data with any one value of spin and parity of the compound level. If the 1381 kev resonance level were indeed 1^+ as Chao thought, both distributions should be isotropic, since this state may be formed by s-wave protons. If these distributions were not due solely to the 1381 kev level, but to interference of this level with another level, as was suggested by the gamma-ray measurements, one would expect the observed distributions to vary as the bombarding energy is varied over the resonance. It is to be noted from the observed

distributions that there is fore and aft symmetry ($\pm$ 10 percent). In an attempt to discern any possible interference effects the bombarding energy was set at both $E_R \pm \Gamma/2$, where E_R is the resonance energy (1381 kev) and Γ is the total width of the gamma-ray excitation curve at half-maximum in energy units. Only a few points were run at each energy for each group; the results are given in table II.

TABLE II

E	Group	Yield(normalized to unity at 90°) x = 0	x = 1/2	x = 7/8
$E_R + \Gamma/2$	α_2	1	0.96	0.85
$E_R - \Gamma/2$	α_2	1	0.57	0.53
$E_R + \Gamma/2$	α_3	1	0.87	----
$E_R - \Gamma/2$	α_3	1	1.09	----

The only large change which occurs is in the α_2 angular distribution at $E_R + \Gamma/2$; the other changes are within the probable error. Thus interference effects are possible, but are not clearly manifested on the basis of this data.

From the elastic scattering of protons done in this laboratory, it is known that this level has odd parity, and that the distribution can be fitted on the assumption of the formation by p-wave protons. Thus it seems probable that this is a 2^- level. This assignment has also been obtained by Sanders[21], who managed to separate the 6.14 Mev gamma-ray from the 6.91 and 7.12 Mev gamma-rays, using a deuterium filled ionization chamber. He measured the angular distribution of the 6.14 Mev gamma-ray by itself, and the combination of the 6.91 and 7.12 Mev gamma-rays together. The distributions were fitted with curves of

the form $1 + a \cos^2\theta$, where $a = -0.14 \pm 0.03$ for γ_1 and 0.58 ± 0.13 for $\gamma_2 + \gamma_3$. This led him to the 2^- assignment for the level. Also, he measured the ratio $\gamma_1/(\gamma_2 + \gamma_3)$, and using the theoretical distributions, obtained the same distribution as Day et al.[23] for the combination of the three gamma-rays.

Thus the assignment to the level seems firmly established, and the only question left is, to what is the change in the alpha particle distributions due? One factor which modifies the distributions is the contribution of higher ℓ values. One might almost get the α_2 distribution in this way, but too much $\cos^4\theta$ would be introduced into the α_3 distribution to have gone unnoticed. In addition, the value of $W(x)$ must always rise to 2 when $x = 1$ for the α_3 distribution no matter what values are assumed for A and cos α. It might be noticed that there is some indication of a small amount of $\cos^4\theta$ in the α_2 distribution. This would be compatible with the contribution of higher ℓ values. However, the data does not warrant an exact fitting to obtain the coefficient of a possible $\cos^4\theta$ term.

Another factor which would move the distributions in the observed direction would be the presence of a constant background, with little interference. At 1400 kev bombarding energy the α_2 yield was observed to be about 5 percent of the α_2 yield at the resonance; the α_3 yield was about 10 percent of that at the resonance. These values are nowhere near large enough to produce the observed distributions, however. The level, non-resonant background in this region has been thought to be 0^+.[1]

A third factor which can appreciably modify distributions is interference. The nearest known levels to the 1381 kev resonance are the

2^- level at 1355 kev, a 2^+ long-range alpha particle and pair resonance at 1367 kev, a capture resonance at 1431 kev (1^+), and finally the non-resonant background (thought to be 0^+). The gamma-ray yield curve in this region is shown in fig. 18; other measurements have shown that the small peak at 1.42 Mev must be due to soft radiation, and is not from the gamma-ray emitting levels in O^{16}.

If interference with the 2^- level is considered, it is found difficult to fit the observed data. Interference between the two 2^- levels gives the same distribution as either level by itself with only the intensity being modified. Interference with the 2^+ level would give terms in cos θ and $\cos^3\theta$, which does not agree with the fore and aft symmetry observed. However, this fore and aft symmetry was observed at only one bombarding energy, and it is conceivable that at just this point the coefficient of these terms was small. If this possibility is considered, then the interference pattern with these terms removed can not possibly fit the observed distributions. For the same reason interference with the 1^+ level does not give agreement with the data. Also the 0^+ level would give terms in cos θ. Due to the uncertainty in the assignment to this background, the pattern from either a 1^- level or 3^- level interfering with the 2^- level were considered. Since these states have the same parity as the state with which they interfere these distributions had the observed fore and aft symmetry. However, neither reproduced the observed results very closely, although the 1^- level moved the distributions in the right direction. It seems that more complete data is required to reach a definite conclusion. In particular, a very useful bit of information would be the angular distribution of the α_1 group at this energy. Since this group is so intense background

effects would be minimized. A range of distributions for several energies would be useful, in addition to complete forward angle data. Also, the angular correlation between the alpha particle groups and the de-excitation gamma-rays would be very helpful.

3. Q-values and Cross Sections of the Reaction $F^{19}(p\ p')F^{19*}$

The two inelastic proton groups corresponding to the two lowest known excited levels of F^{19} were first observed at the 1381 kev resonance level, at 160 degrees in the laboratory system. After checking that these were the right groups by observing how they moved with changes in the angle of observation and bombarding energy, a brief excitation curve was run from just below 1355 kev to about 1500 kev. Both groups were observed to follow the well-known resonances at 1355 and 1381 kev, and in addition, there was a much stronger resonance for the first group at 1431 kev, which had not previously been reported as a resonance. The group corresponding to the first excited level was about twenty times as intense as that due to the second excited level. During this work, a preprint from the Rice Institute[24] reported this as a capture gamma-ray resonance. The running of excitation curves for the protons was halted here, as the gamma-rays from the de-excitation of these two levels were being observed concurrently, and it was a much simpler task to observe the resonances for inelastic scattering from the gamma-ray yield. The gamma-ray energy remains constant as the bombarding energy is changed, whereas the proton energy varies, and the spectrometer setting must be determined for each energy used.

The two groups were observed at several bombarding energies and angles during the course of this work, and from this data the Q-values of the reactions calculated. The resultant values for the energies of the

first two excited levels are 113.9 ± 0.8 and 199.6 ± 0.7 kev, in agreement with the energy measurements on the accompanying gamma-rays.[25] These values are the result of 14 measurements on the first level and 25 measurements on the second level.

The cross sections for the inelastic scattering processes were measured at two bombarding energies. The method of determining these cross sections was as follows: the fluorine elastic peak was observed, along with the inelastic peaks, and the total area under each of these peaks calculated graphically. The cross section for each of these processes then goes as this number divided by the fluxmeter reading at the peak. The ratio of A to I (where A is the area under the peak) for one group is to the same ratio for another group as the ratio of their differential cross sections, since all other factors remained constant (target thickness, solid angle, and amount of bombardment). The absolute cross section for the elastic scattering was obtained from the work done in this laboratory, which then gave the absolute differential cross sections for the inelastic scattering processes. The values obtained in this manner were in good agreement with those obtained from the gamma-ray yields.[25]

The cross sections for both groups were measured at the 1431 kev resonance. The measurements were made at 159.7 degrees in the laboratory system; as will be seen in the angular distribution work, the distribution of the first group was isotropic. This result is supported by the work on the elastic scattering of protons, which indicated that this Ne^{20} resonance level has spin and parity 1^+. Since the level may be formed by s-wave protons both distributions are expected to be isotropic. Then the differential cross sections need only be multiplied by 4π to get the total

cross sections. The resulting cross sections were 0.187 ± 0.015 barns for the group corresponding to the first excited level, and 0.007 ± 0.002 barns for the second group. The second group was so weak that accurate measurements were difficult, and thus the cross section is only given to one significant figure.

At the 1381 kev resonance the yield of the second group was measured at 90 degrees in the laboratory system, and compared with the elastic yield. In this case the angular distributions indicated a distribution of the form $1 + a \cos^2\theta$, and therefore the differential cross section at 90 degrees was multiplied by the factor $4\pi\ (1 + a/3)$ (where $a = -0.45$) to get the total cross section. This gave 0.0427 ± 0.0040 barns as the cross section for the second group.

4. Angular Distributions of the Reaction $F^{19}(p\ p')F^{19*}$

The results of the angular distribution measurements are listed in table III. All distributions were fitted with curves of the form $1 + a \cos^2\theta$; these coefficients a are listed, a_1 referring to the first group and a_2 to the second.

TABLE III

Coefficients in the Angular Distributions $1 + a \cos^2\theta$ for the Reaction $F^{19}(p\ p')F^{19*}$

E_p(kev)	a_1	a_2
874	----	0 ± 0.1
1355	----	0 ± 0.1
1381	----	-0.45 ± 0.04
1431	0 ± 0.1	----

The angular distribution data is meager, due to the difficulties

involved in getting the groups free of unwanted elastic peaks. Fig. 19 shows a profile run across the region in question at a bombarding energy of 1431 kev and at the angle 159.7 degrees. The elastic peaks become larger at smaller scattering angles and lower energies, making it quite difficult to observe the inelastic groups. Thus, while it was always possible to observe a group at one angle, it was not always possible to obtain it again at another angle and get the angular distribution. The group corresponding to the first F^{19} excited level was the most difficult to observe, it being so close to the elastic peak due to carbon everywhere. However, two points were obtained at the 1431 kev resonance, at 90 and 159.7 degrees, which indicated that the distribution was isotropic to $\pm$ 10 percent. As mentioned above, this is in agreement with the elastic scattering.

The number of resonances available to an experimenter trying to determine the spin and parity of these two excited states in F^{19} was severely restricted. All of the known resonance levels in Ne^{20} which gave the two groups had spin assignments of either 1^+ or 2^-. Since the 1^+ level may be formed by s-wave protons, any distribution obtained from these levels will be isotropic. The three useful levels were the 874 (which gave almost no protons corresponding to the first excited state), the 1355 and the 1381 kev resonance levels, all with 2^- assignments.

The distribution of the protons corresponding to the second excited level in F^{19} was measured at 1381 kev, and the result $1 - 0.45 \cos^2\theta$ obtained. At bombarding energies of both 874 and 1355 kev, isotropic distributions were obtained. The points taken at each resonance were few, as is shown in figs. 20-22, due to the afore-mentioned difficulties, and the results are only good to about $\pm$ 10 percent.

Since a thorough job could not be done on the angular distributions, no assignments can be made on the basis of the particle work alone. In addition, all distributions are ambiguous due to the presence of the proton spin, making the addition of an arbitrary factor necessary in each. However, work on the gamma-rays[25,26,27], including angular distributions and lifetime measurements, have led to an assignment of $5/2^+$ for the upper level. As can be seen from the theoretical particle angular distributions in Appendix II, the three observed angular distributions are consistent with a $5/2^+$ assignment for the second level. One extreme solution has the coefficient 1/3, the other -7/9. Since the resulting distribution may be any linear combination of these two, it is readily seen that isotropy or a coefficient -0.45 are possible distributions from a $5/2^+$ level.

The only distribution observed of protons corresponding to the first excited level was explained solely on the basis of the spin and parity of the Ne^{20} resonance level (1^+ at 1431 kev) and gave no information as to the spin and parity of the first excited level.

V. SUMMARY

The search for a 2^- level in O^{16} has resulted in the region of excitation energy from about 7 to 9 Mev being covered, with no new levels discovered. Whether or not such a level would appear in another reaction was of course not decided.

The angular distributions themselves have led to only one new assignment for the Ne^{20} resonance levels; that of 2^- to the 1355 kev resonance level. All other distributions were in agreement with previous assignments, or with those made subsequently on the basis of the elastic scattering. The only exception was at 1381 kev, where no definite conclusion could be drawn. It seems likely that interference effects were

modifying the distributions, but no definite conclusion as to the interfering level or levels could be drawn.

The study of the inelastic protons from the $F^{19}(p\ p')F^{19*}$ reaction gave the energies of the first two known levels of F^{19} to be 113.9 ± 0.8 and 199.6 ± 0.7 kev. The cross sections for the first and second groups at the 1431 kev resonance were 0.187 ± 0.015 and 0.007 ± 0.002 barns, respectively. At 1381 kev, the cross section for the second group was 0.0427 ± 0.0040 barns.

Those angular distributions which were obtained were not sufficient to make unique spin and parity assignments to either final state, but all distributions measured were consistent with assignments made on the basis of the gamma-ray work.

References

1. Chao, Tollestrup, Fowler, and Lauritsen, Phys. Rev. 79, 108 (1950).
2. J. A. Wheeler, Phys. Rev. 52, 1083 (1937); Wheeler and Teller, Phys. Rev. 53, 778 (1939); Hafstad and Teller, Phys. Rev. 54, 681 (1938).
3. D. M. Dennison, Phys. Rev. 57, 454 (1940).
4. J. Seed and A. P. French, Phys. Rev. 88, 1007 (1952).
5. C. Y. Chao, Phys. Rev. 80, 1035 (1950).
6. Cowie, Heydenburg, and Phillips, Phys. Rev. 87, 304 (1952).
7. Bender et al., private communication to T. Lauritsen; see Revs. Modern Phys. 24, 321 (1952).
8. C. Mileikowsky and W. Whaling, Phys. Rev. 88, 1254 (1952).
9. R. B. Day, private communication.
10. D. R. Inglis, Revs. Modern Phys. 25, 390 (1953).
11. E. U. Condon and G. H. Shortley, The Theory of Atomic Spectra, Cambridge University Press, Cambridge, 1935 and 1951.
12. A. A. Kraus, Ph.D. Thesis, C. I. T. (1953).
13. J. M. Blatt and L. C. Biedenharm, Revs. Modern Phys. 24, 258 (1952).
14. L. C. Biedenharm, Oak Ridge Nat'l. Lab. Reports ORNL-1501 (1953), and ORNL-1098 (1952).
15. G. Racah, Phys. Rev. 62, 438 (1942).
16. Fowler, Lauritsen, and Lauritsen, Revs. Modern Phys. 20, 236 (1948).
17. T. W. Bonner and J. E. Evans, Phys. Rev. 73, 666 (1948).
18. Snyder, Rubin, Fowler, and Lauritsen, Rev. Sci. Inst. 21, 852 (1950).
19. Thomas, Rubin, Fowler, and Lauritsen, Phys. Rev. 75, 1612 (1949).
20. H. Fulbright and R. Bush, Phys. Rev. 74, 1323 (1948).

21. J. E. Sanders, Phil. Mag. 44, 1302 (1953).

22. H. A. Bethe, Revs. Modern Phys. 9, 177 (1937).

23. Day, Chao, Fowler, and Perry, Phys. Rev. 80, 131 (1950).

24. R. M. Sinclair, Phys. Rev. 93, 1082 (1954).

25. Peterson, Barnes, Fowler, and Lauritsen, Phys. Rev. (in press).

26. Barnes, Thirion, and Lauritsen, Phys. Rev. (in press).

27. Sherr, Li, and Christy, Phys. Rev. (in press).

APPENDIX I.

Theoretical Angular Distributions of the $F^{19}(p\,\alpha)O^{16*}$ Reaction (for Ne^{20} $1^+,1^-,2^+,2^-,3^+$, and 3^- levels to O^{16} $1^-,2^-,2^+$, and 3^- levels).

$[\ell,J;\ell',J']$	Distribution
$[0(2),1;1,1]$	$1 + \frac{1}{\sqrt{2}} A \cos\alpha\,(-1+3x) + \frac{1}{8}A^2(41-39x)$
$[0(2),1;1(3),2]$	$1+B^2+\frac{1}{5\sqrt{2}}A\cos\alpha\,(1+2\sqrt{6}B\cos\beta+4B^2)(1-3x) + \frac{A^2}{200}\left[(127+39x)+78\sqrt{6}B\cos\beta\,(1-3x)+4B^2(22+39x)\right]$
$[0(2),1;2,2]$	$1 + \frac{1}{2\sqrt{2}} A \cos\alpha\,(-1+3x) + \frac{3}{80}A^2(23-13x)$
$[0(2),1;3,3]$	$1 + \frac{3}{4\sqrt{2}} A \cos\alpha\,(-1+3x) + \frac{1}{160}A^2(151-117x)$
. . . . .	. . . . .
$[1,1;0,1]$	1
$[1,1;2,2]$	$(1+x)+2C(1-x)$
$[1,1;1,2]$	$(7-x)+2C(3+x)$
$[1,1;2,3]$	$(5-x)+2C(2+x)$
. . . . .	. . . . .
$[2,2;1,1]$	$3(1+x)+2C(1+3x)$
$[2,2;1,2]$	$(5-3x)+6C(1-x)$
$[2,2;0,2]$	1
$[2,2;1,3]$	$(34+16x)+9C(1-x)$

$[\ell,J;\ell',J']$ Distribution

$[1(3),2;2,1]$ $1+x+2\sqrt{\frac{2}{3}}A\cos\alpha(1-9x+10x^2)+\frac{2}{3}A^2(1+6x-5x^2)$

$[1(3),2;0(2),2]$ $1+\sqrt{\frac{7}{10}}B\cos\beta(1-3x)+\frac{1}{28}B^2(31-9x)$

$+\sqrt{6}A\cos\alpha\left[\sqrt{\frac{2}{35}}B\cos\beta(-1+3x)+\frac{3}{14}B^2(-1+9x-10x^2)\right]$

$+A^2\left[1+4\sqrt{\frac{2}{35}}B\cos\beta(1-3x)+\frac{1}{14}B^2(17-18x+15x^2)\right]$

$[1(3),2;1(3),2]$ $1-\frac{7}{9}x+\frac{4}{9}B\cos\beta(1-3x)+\frac{2}{9}B^2(3+x)$

$+\frac{2}{9}\sqrt{\frac{2}{3}}A\cos\alpha\left[(-1+3x)+2B\cos\beta(-3+24x-25x^2)\right.$

$\left.+\frac{1}{2}B^2(7-66x+75x^2)\right]$

$+\frac{4}{27}A^2\left[(7-6x)+\frac{1}{2}B\cos\beta(9-42x+25x^2)+\frac{1}{8}B^2(29+78x-75x^2)\right]$

$[1(3),2;2(4),3]$ $1-\frac{2}{3}x+\frac{1}{3}\sqrt{\frac{5}{2}}B\cos\beta(1-3x)+\frac{1}{12}B^2(9+x)$

$+\frac{1}{6\sqrt{6}}A\cos\alpha\left[(-1-6x+15x^2)+4\sqrt{\frac{5}{2}}B\cos\beta(-3+24x-25x^2)\right.$

$\left.+2B^2(4-39x+45x^2)\right]$

$+\frac{1}{72}A^2\left[(73-42x-15x^2)+4\sqrt{\frac{5}{2}}B\cos\beta(9-42x+25x^2)\right.$

$\left.+2B^2(23+42x-45x^2)\right]$

. . . . . .

$[2,3;3,1]$ $\quad 5 + 6x + 5x^2$

$[2,3;1,2]$ $\quad 23 + 36x$

$[2,3;2,2]$ $\quad 35 + 162x - 165x^2$

$[2,3;1,3]$ $\quad 10 - 9x$

$[3,3;2,1]$ $\quad (5 + 6x + 5x^2) + 6C(1 - 2x + 5x^2)$

$[3,3;2,2]$ $\quad (13 + 18x - 15x^2) + 6C(1 + 14x + 15x^2)$

$[3,3;1,2]$ $\quad (7 + 9x) + 6C(1 + 2x)$

$[3,3;0,3]$ $\quad 1$

APPENDIX II.

Theoretical Angular Distributions of the $F^{19}(p\ p')O^{16*}$ Reaction (for a Ne^{20} 2^- level)

Final State in F^{19}	Distribution
$1/2^+$	$13 + 21x$
$1/2^-$	$2(1 + 3x) + 3C(1 + x)$
$3/2^+$	$13 + 21x + 3C(9 - 7x)$
$3/2^-$	$25 - 9x + 28C$
$5/2^+$	$9 - 7x + 2C(3 + x)$
$5/2^-$	$7 + 3C(3 - 2x)$
$7/2^+$	$6(3 + x) + 5C(5 - 3x)$
$7/2^-$	$3 - 2x + C(2 + x)$

LEVEL SCHEME FOR REGION STUDIED IN $F^{19}(p\,\alpha)\,O^{16*}$ REACTION

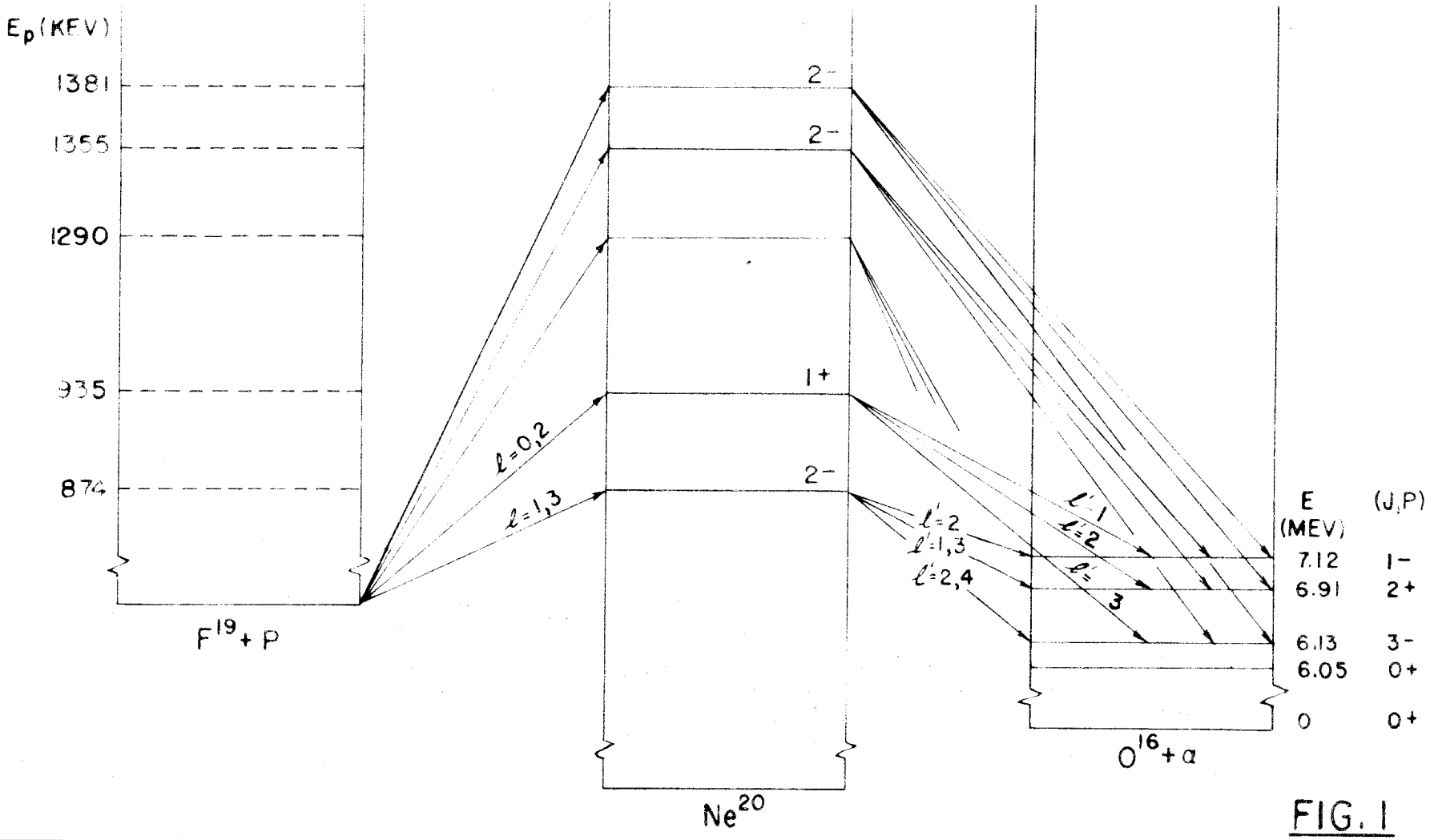

FIG. 1

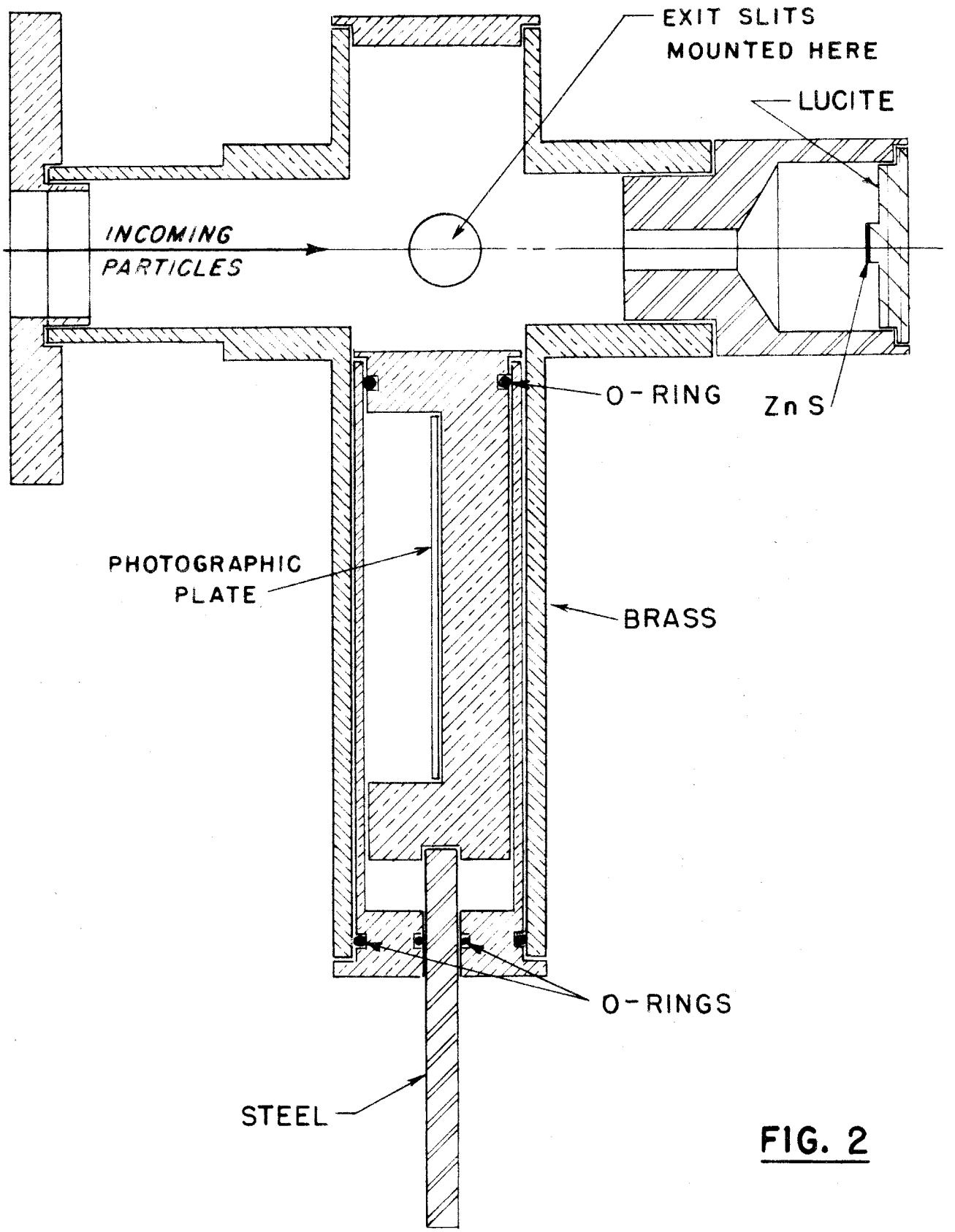

FIG. 2

PLATE HOLDER

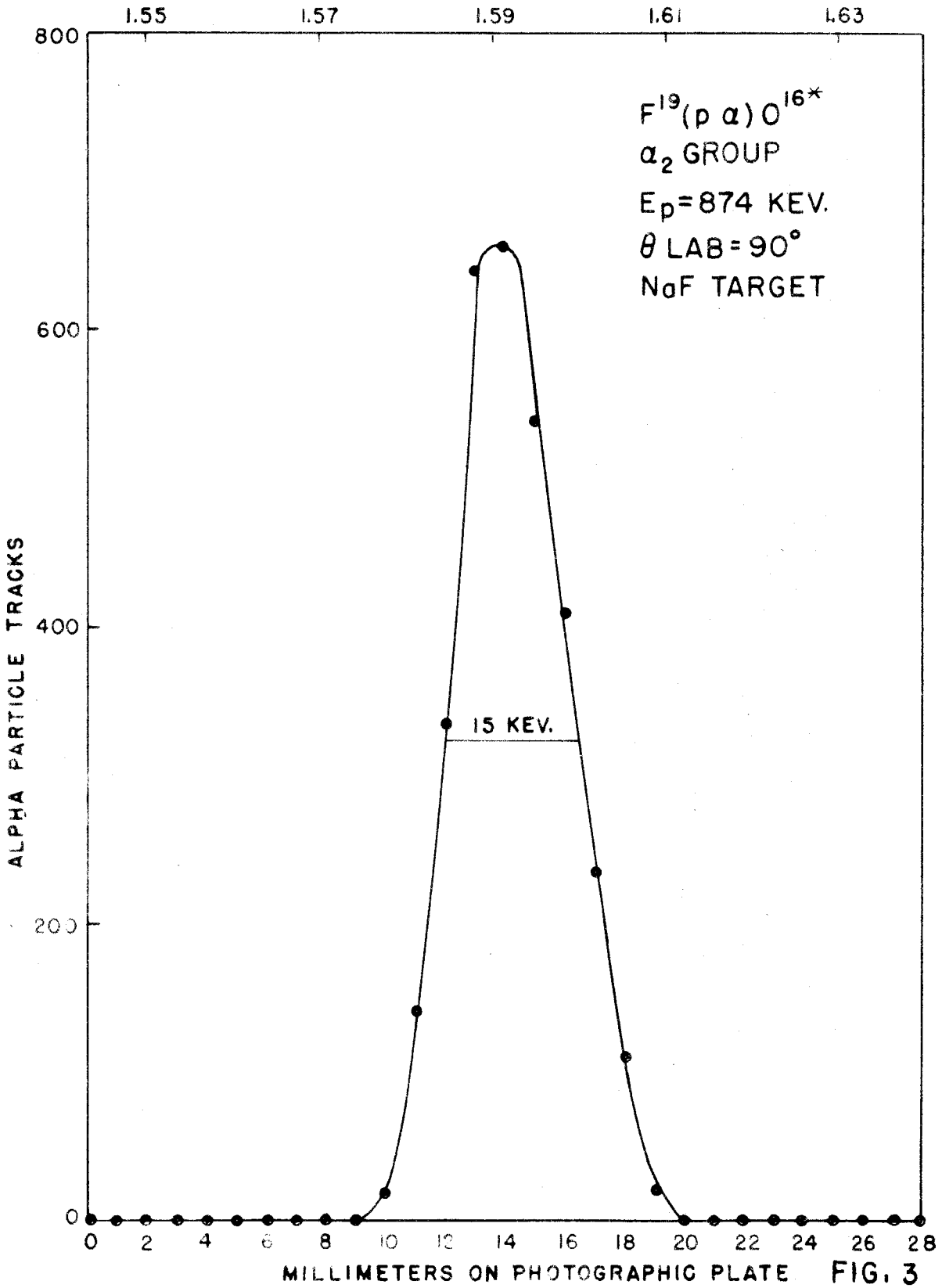
1.55
1.57
1.59
1.61
1.63
800
600
400
200
0
$F^{19}(p\,\alpha)O^{16*}$
α_2 GROUP
E_p=874 KEV.
θ LAB=90°
NaF TARGET
15 KEV.
ALPHA PARTICLE TRACKS
0
2
4
6
8
10
12
14
16
18
20
22
24
26
28
MILLIMETERS ON PHOTOGRAPHIC PLATE

FIG. 3

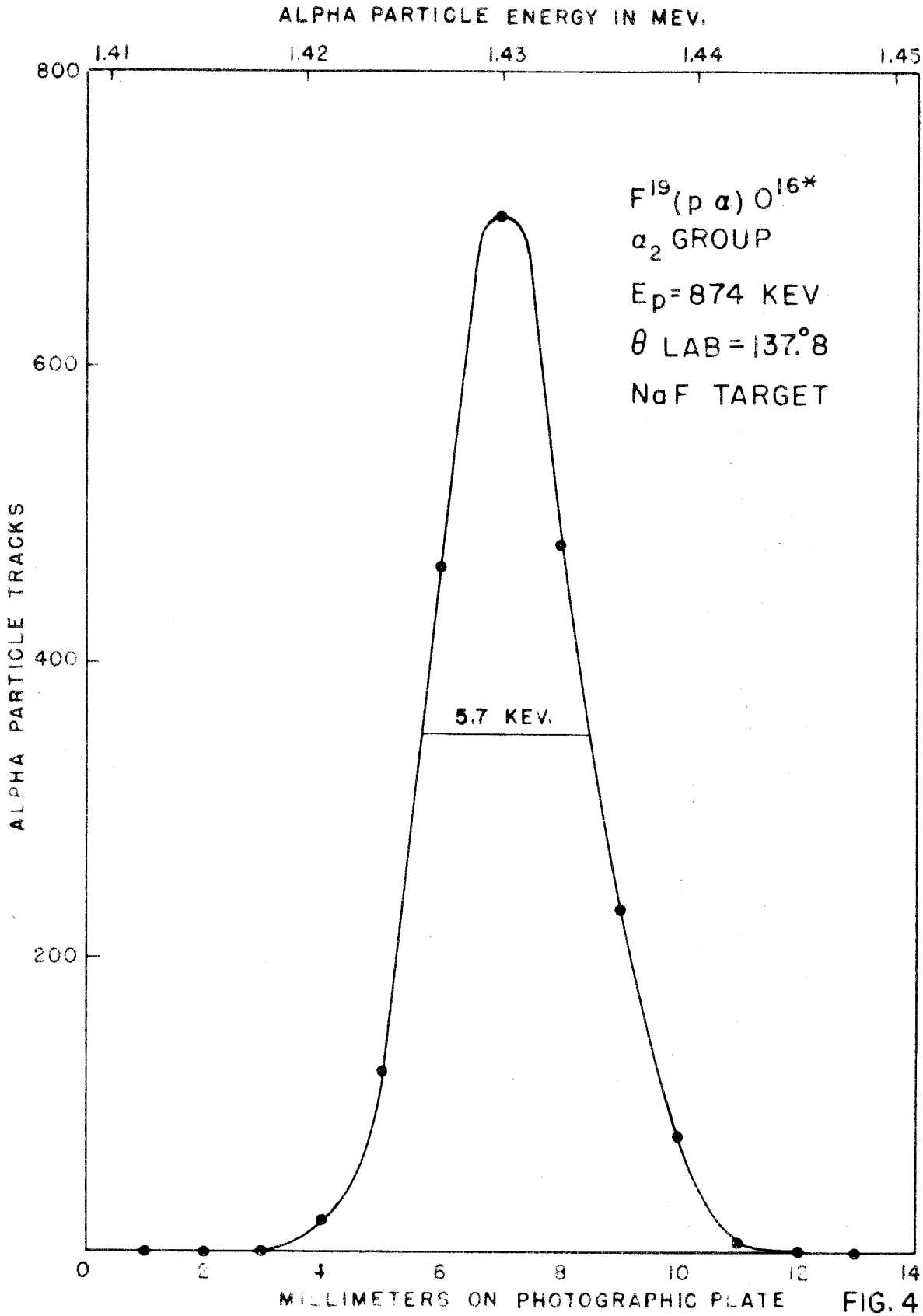
ALPHA PARTICLE ENERGY IN MEV.
1.41
1.42
1.43
1.44
1.45
800
600
400
200
0
2
4
6
8
10
12
14
ALPHA PARTICLE TRACKS
MILLIMETERS ON PHOTOGRAPHIC PLATE
F19(p α) O16*
α2 GROUP
Ep = 874 KEV
θ LAB = 137.°8
NaF TARGET
5.7 KEV.

FIG. 4

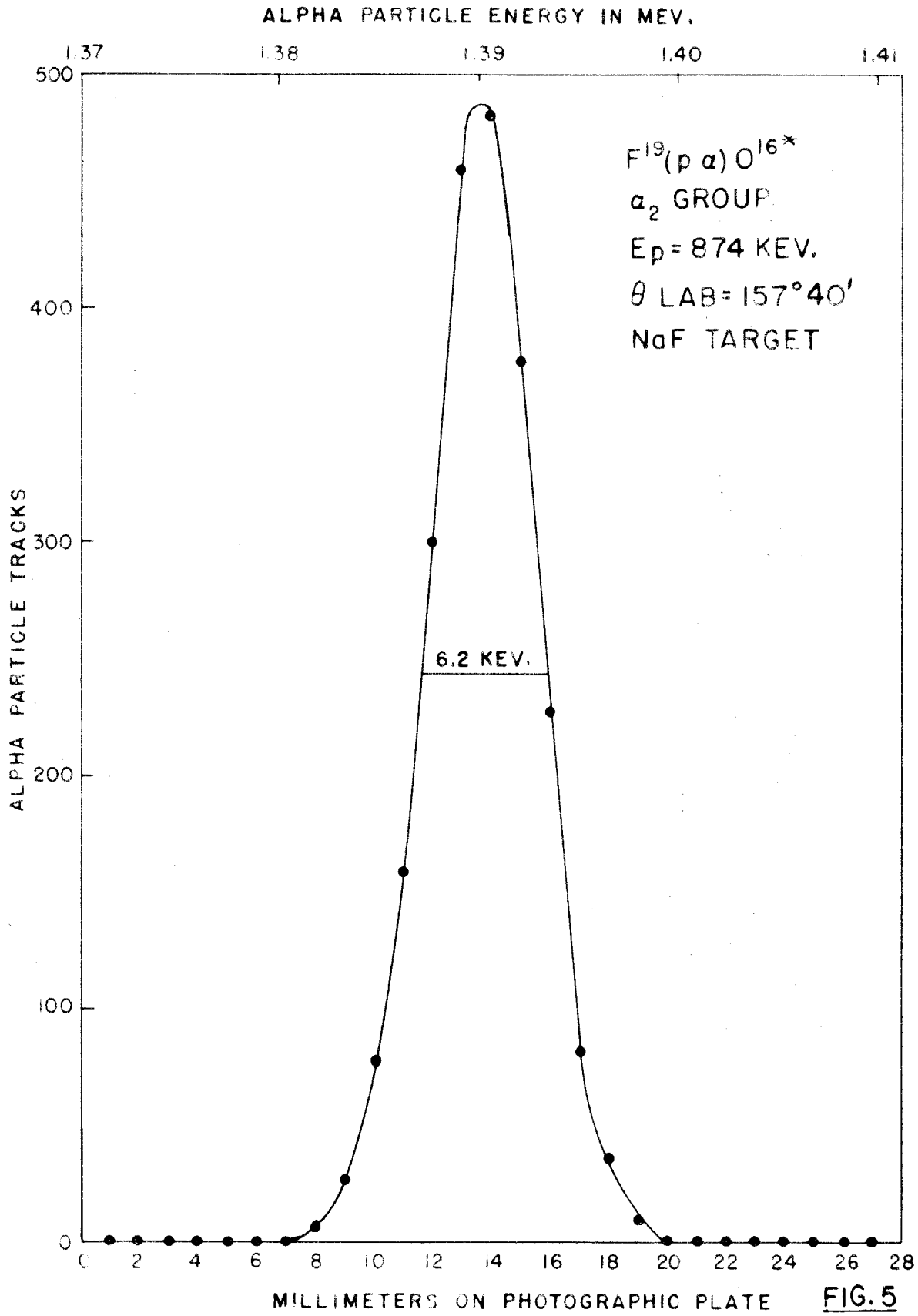
ALPHA PARTICLE ENERGY IN MEV.
1.37
1.38
1.39
1.40
1.41
500
400
300
200
100
0
ALPHA PARTICLE TRACKS
$F^{19}(p\,\alpha)\,O^{16*}$
α_2 GROUP
Ep = 874 KEV.
θ LAB = 157°40'
NaF TARGET
6.2 KEV.
0
2
4
6
8
10
12
14
16
18
20
22
24
26
28
MILLIMETERS ON PHOTOGRAPHIC PLATE

FIG. 5

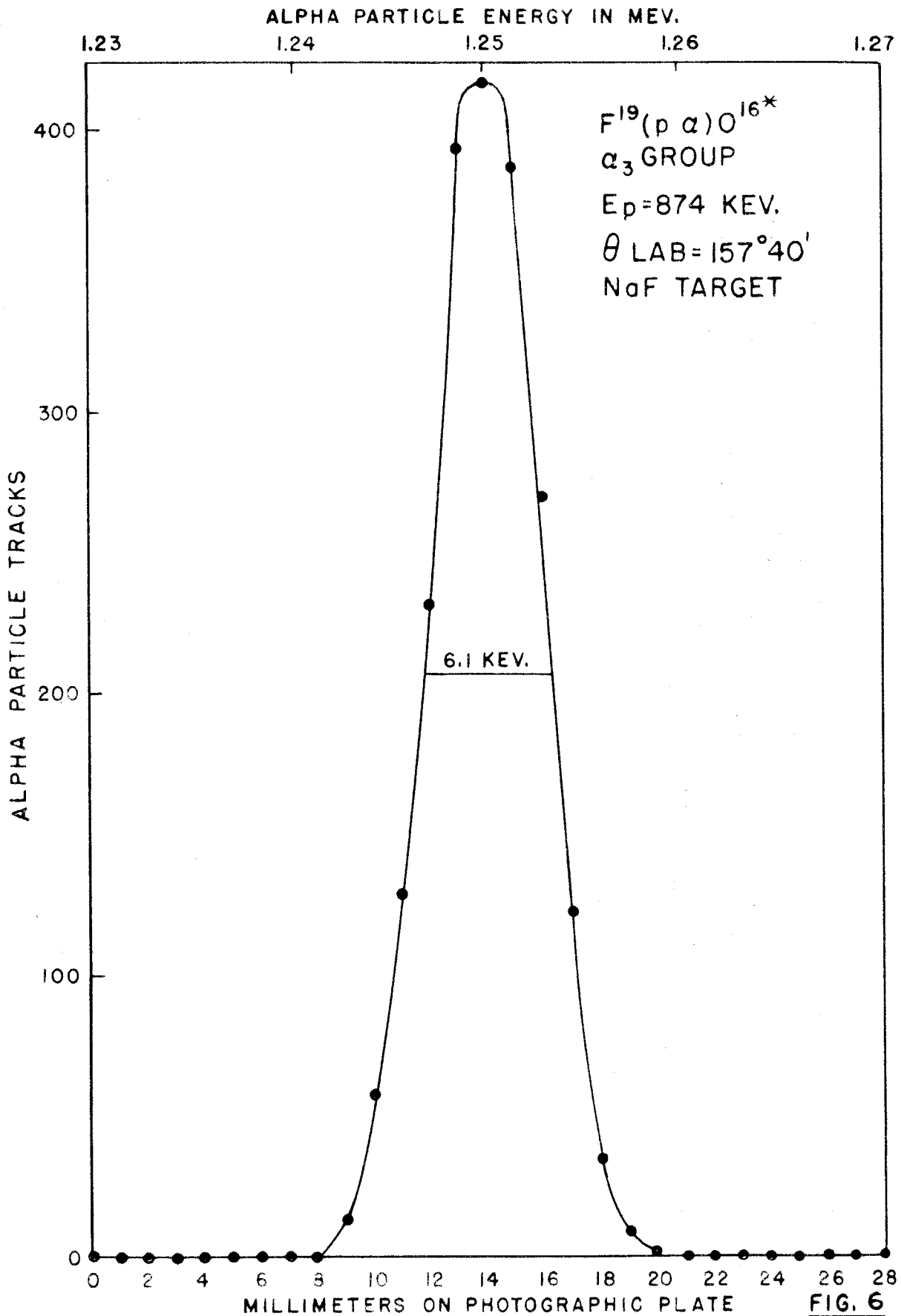
ALPHA PARTICLE ENERGY IN MEV.
1.23
1.24
1.25
1.26
1.27
$F^{19}(p\,\alpha)O^{16*}$
α_3 GROUP
Ep = 874 KEV.
θ LAB = 157°40'
NaF TARGET
6.1 KEV.
ALPHA PARTICLE TRACKS
400
300
200
100
0
0 2 4 6 8 10 12 14 16 18 20 22 24 26 28
MILLIMETERS ON PHOTOGRAPHIC PLATE

FIG. 6

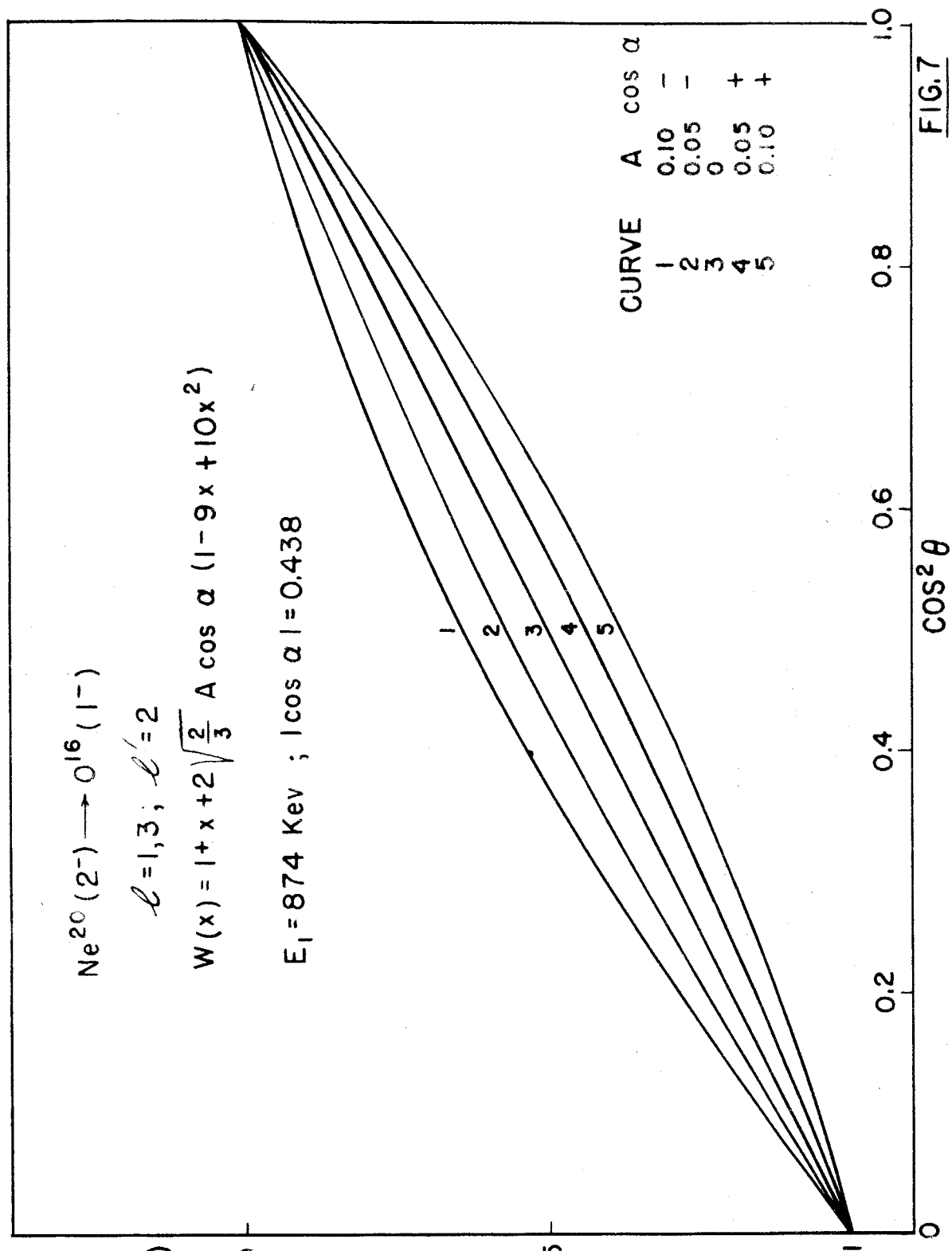
$Ne^{20}(2^-) \longrightarrow O^{16}(1^-)$
$\ell = 1,3\ ;\ \ell' = 2$
$W(x) = 1 + x + 2\sqrt{\frac{2}{3}}\ A \cos\alpha\ (1 - 9x + 10x^2)$
$E_1 = 874$ Kev ; $|\cos\alpha| = 0.438$
CURVE A cos α
1 0.10 −
2 0.05 −
3 0
4 0.05 +
5 0.10 +
W(x)
2.0
1.5
1
0
0.2
0.4
0.6
0.8
1.0
$\cos^2\theta$

FIG. 7

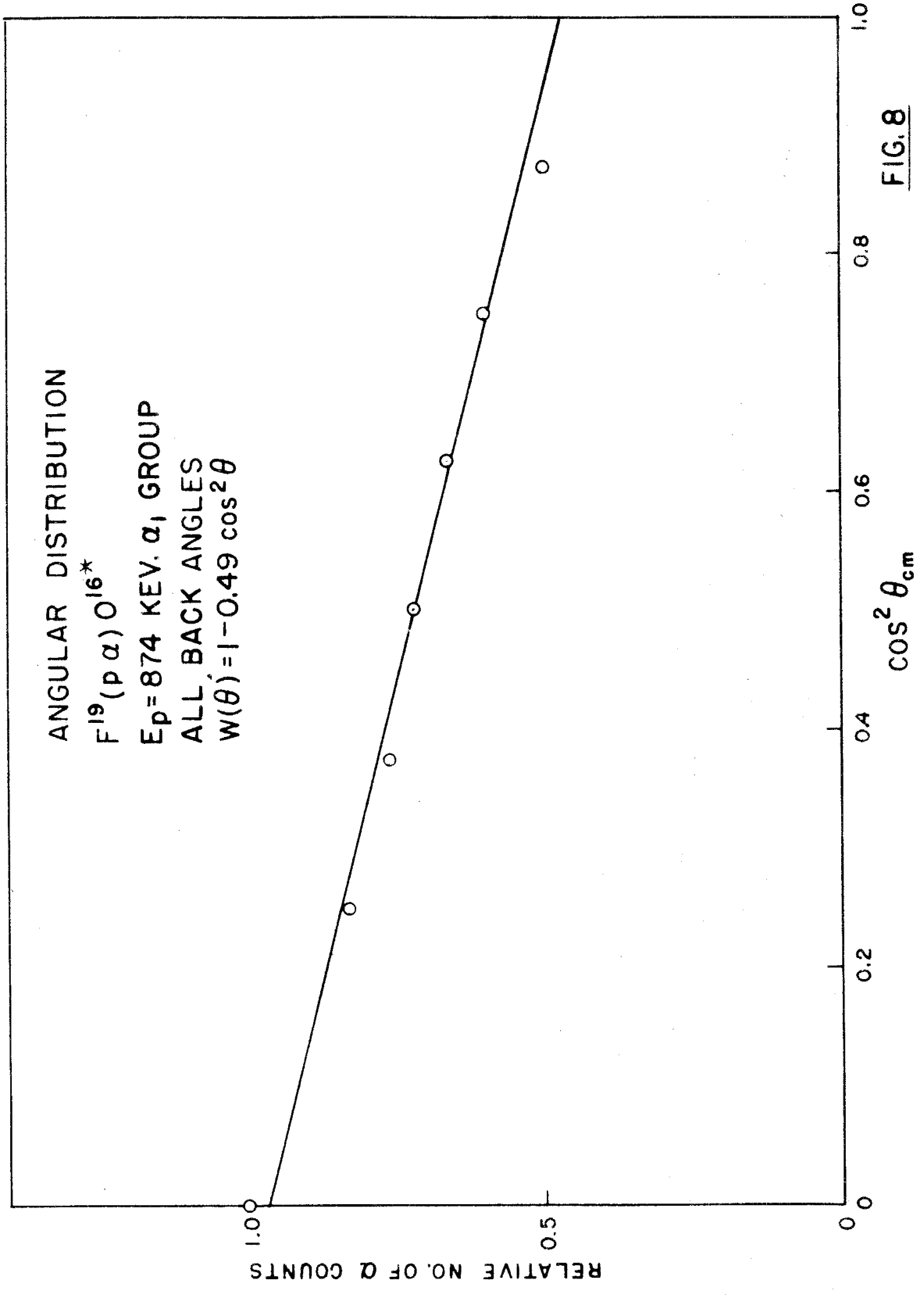
ANGULAR DISTRIBUTION
$F^{19}(p\,\alpha)\,O^{16*}$
E_p = 874 KEV. α_1 GROUP
ALL BACK ANGLES
$W(\theta) = 1 - 0.49\cos^2\theta$
RELATIVE NO. OF α COUNTS
1.0
0.5
0
0
0.2
0.4
0.6
0.8
1.0
$\cos^2\theta_{cm}$

FIG. 8

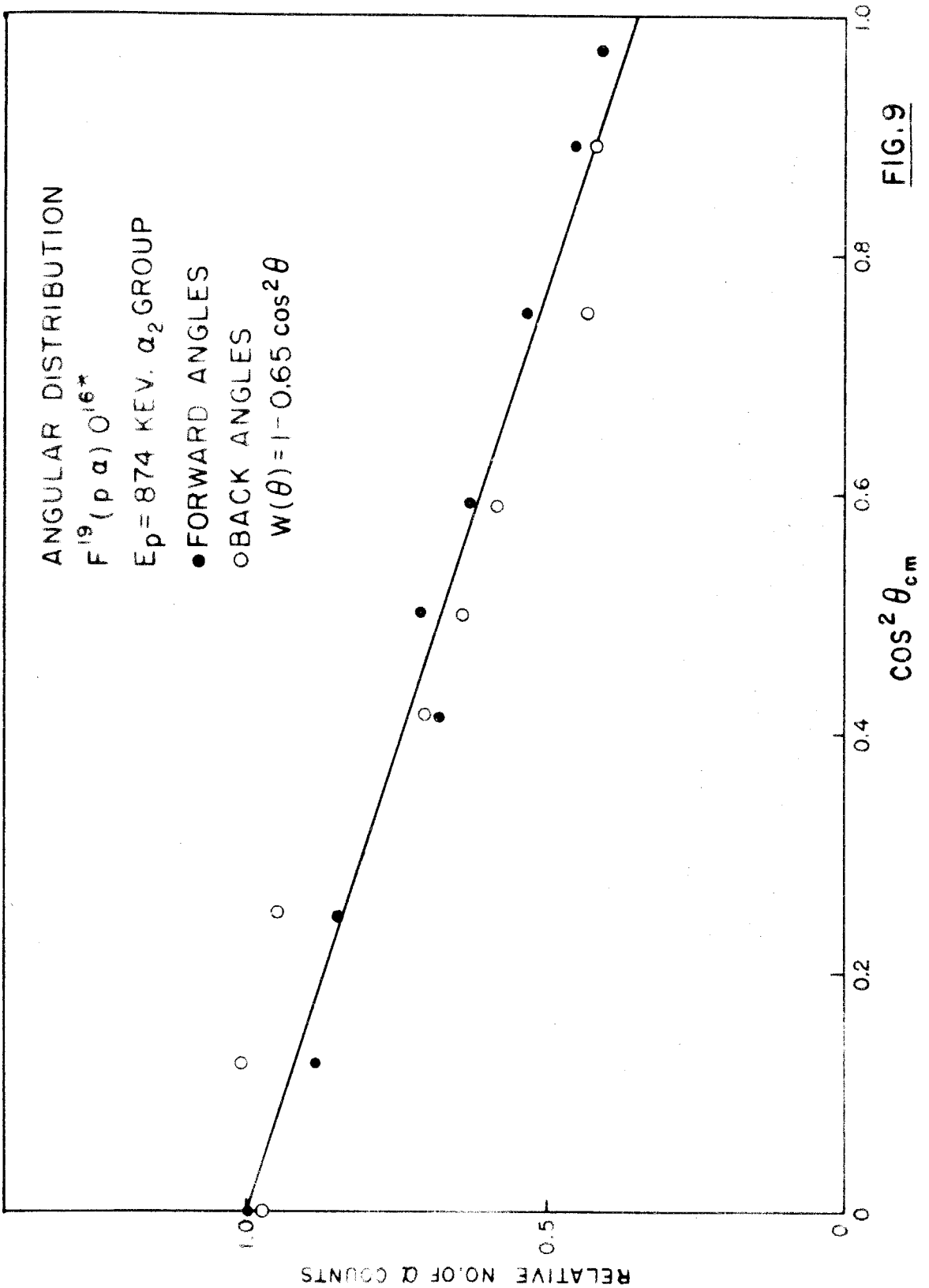
ANGULAR DISTRIBUTION
$F^{19}(p\alpha)O^{16*}$
$E_p = 874$ KEV. α_2 GROUP
● FORWARD ANGLES
○ BACK ANGLES
$W(\theta) = 1 - 0.65\cos^2\theta$
RELATIVE NO. OF α COUNTS
1.0
0.5
0
0
0.2
0.4
0.6
0.8
1.0
$\cos^2\theta_{cm}$

FIG. 9

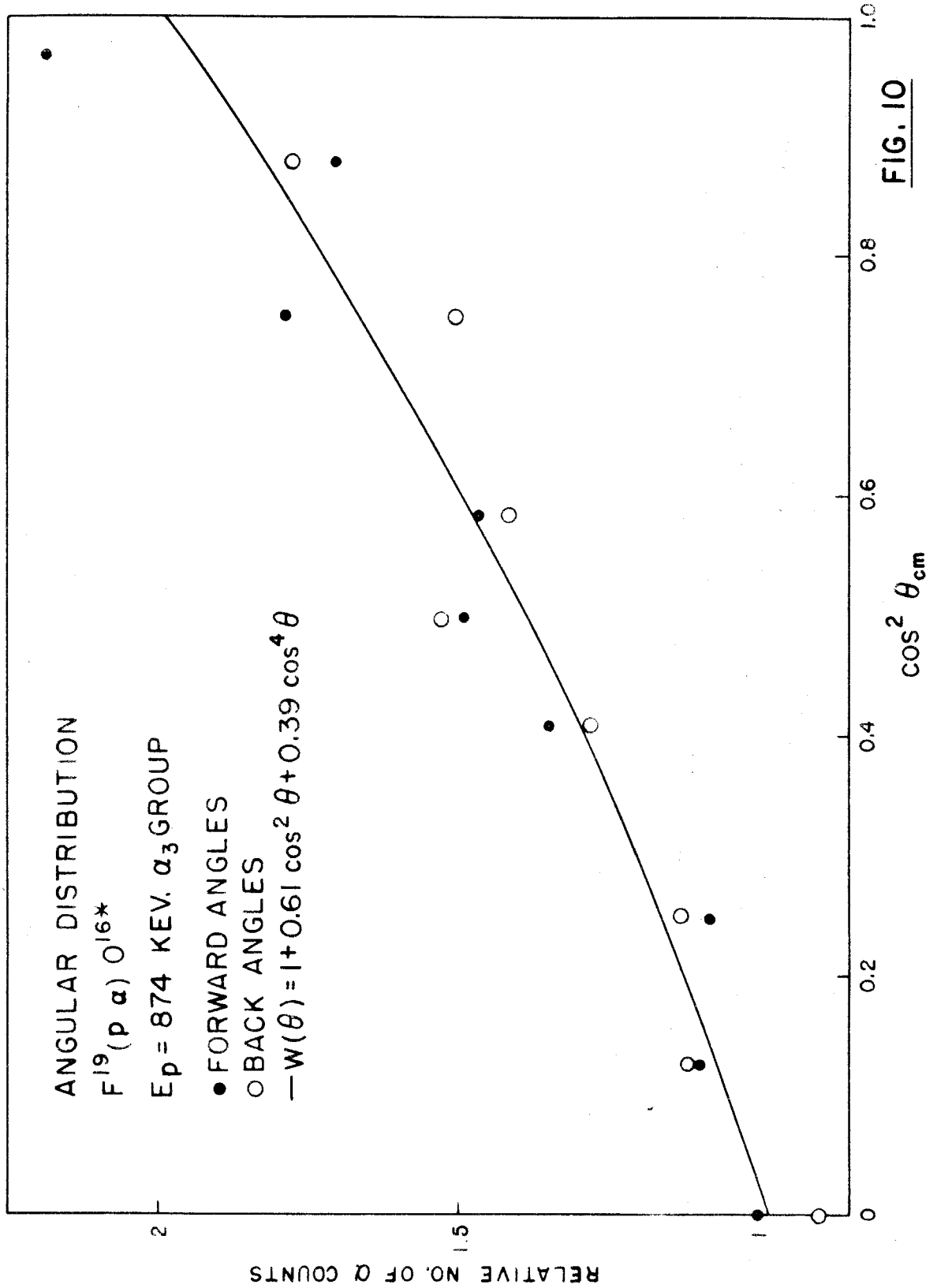
ANGULAR DISTRIBUTION
$F^{19}(p\ \alpha)\ O^{16*}$
$E_p = 874$ KEV. α_3 GROUP
● FORWARD ANGLES
○ BACK ANGLES
$-W(\theta) = 1 + 0.61\cos^2\theta + 0.39\cos^4\theta$
RELATIVE NO. OF α COUNTS
1
1.5
2
0
0.2
0.4
0.6
0.8
1.0
$\cos^2\theta_{cm}$

FIG. 10

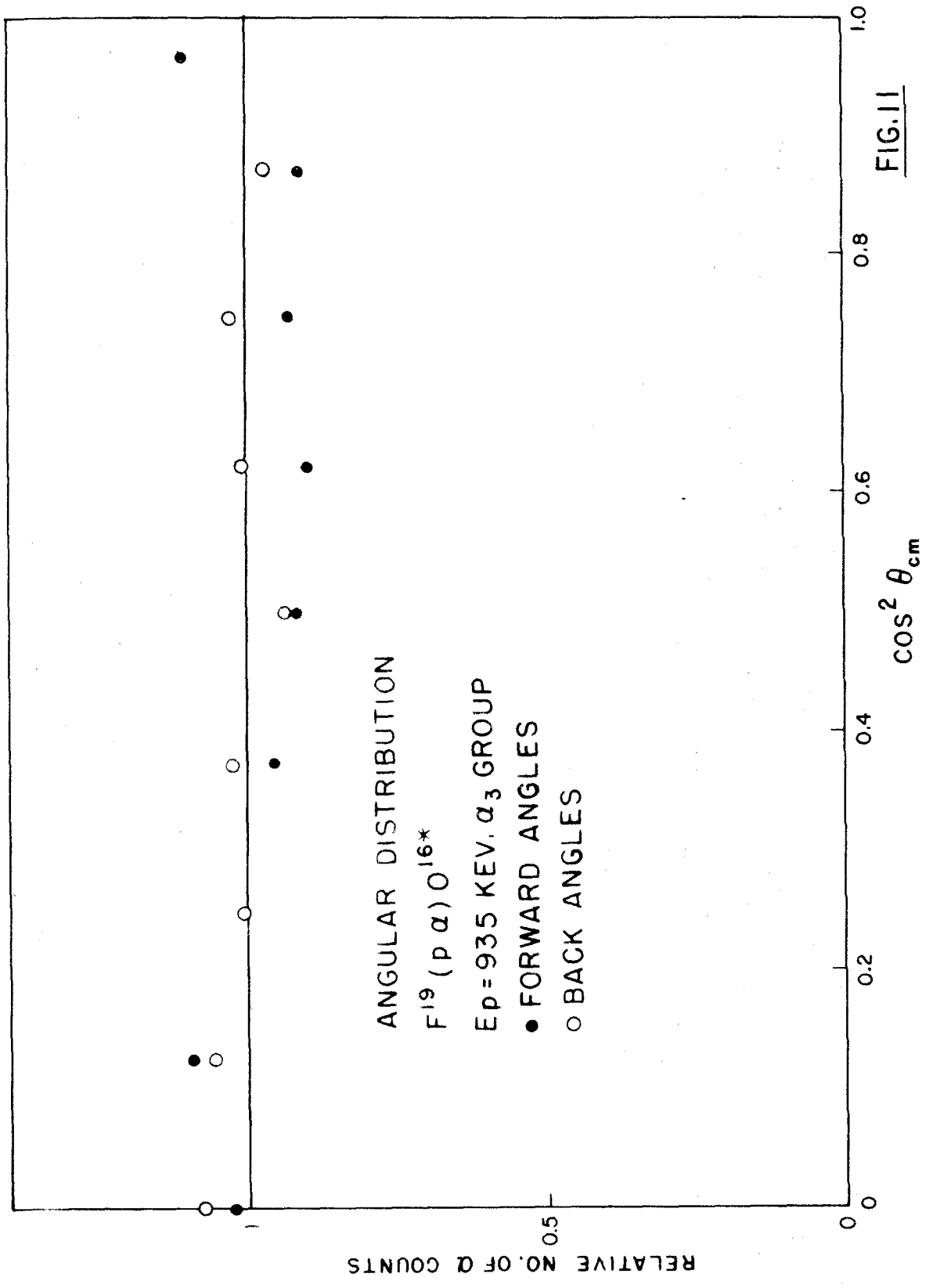
ANGULAR DISTRIBUTION
$F^{19}(p\,\alpha)\,O^{16*}$
Ep = 935 KEV. α_3 GROUP
● FORWARD ANGLES
○ BACK ANGLES
RELATIVE NO. OF α COUNTS
0
0.5
1
0
0.2
0.4
0.6
0.8
1.0
$\cos^2\theta_{cm}$

FIG. 11

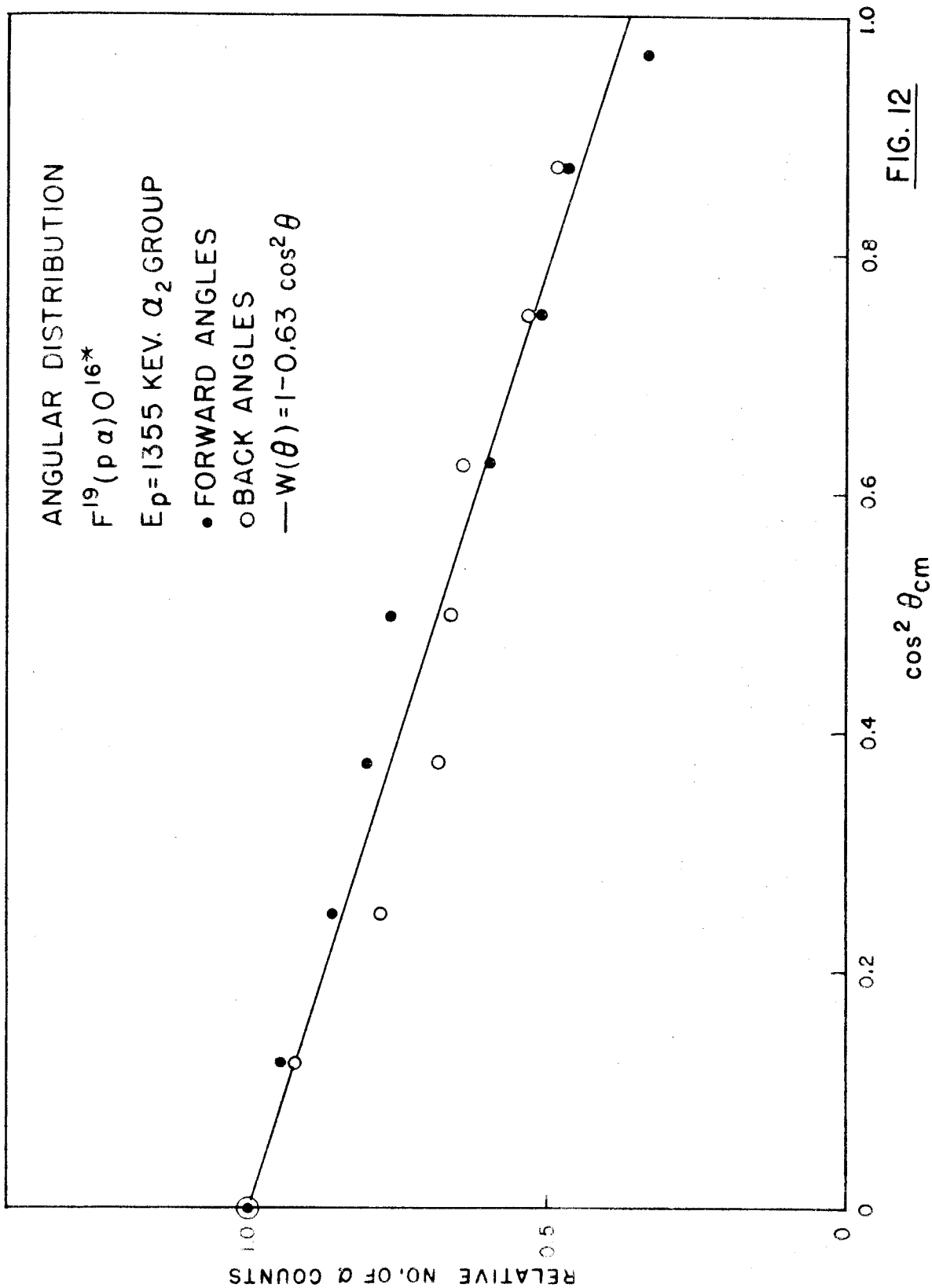
ANGULAR DISTRIBUTION
$F^{19}(p\alpha)O^{16*}$
E_p=1355 KEV. α_2 GROUP
• FORWARD ANGLES
○ BACK ANGLES
— $W(\theta)=1-0.63\cos^2\theta$
RELATIVE NO. OF α COUNTS
1.0
0.5
0
0
0.2
0.4
0.6
0.8
1.0
$\cos^2\theta_{cm}$

FIG. 12

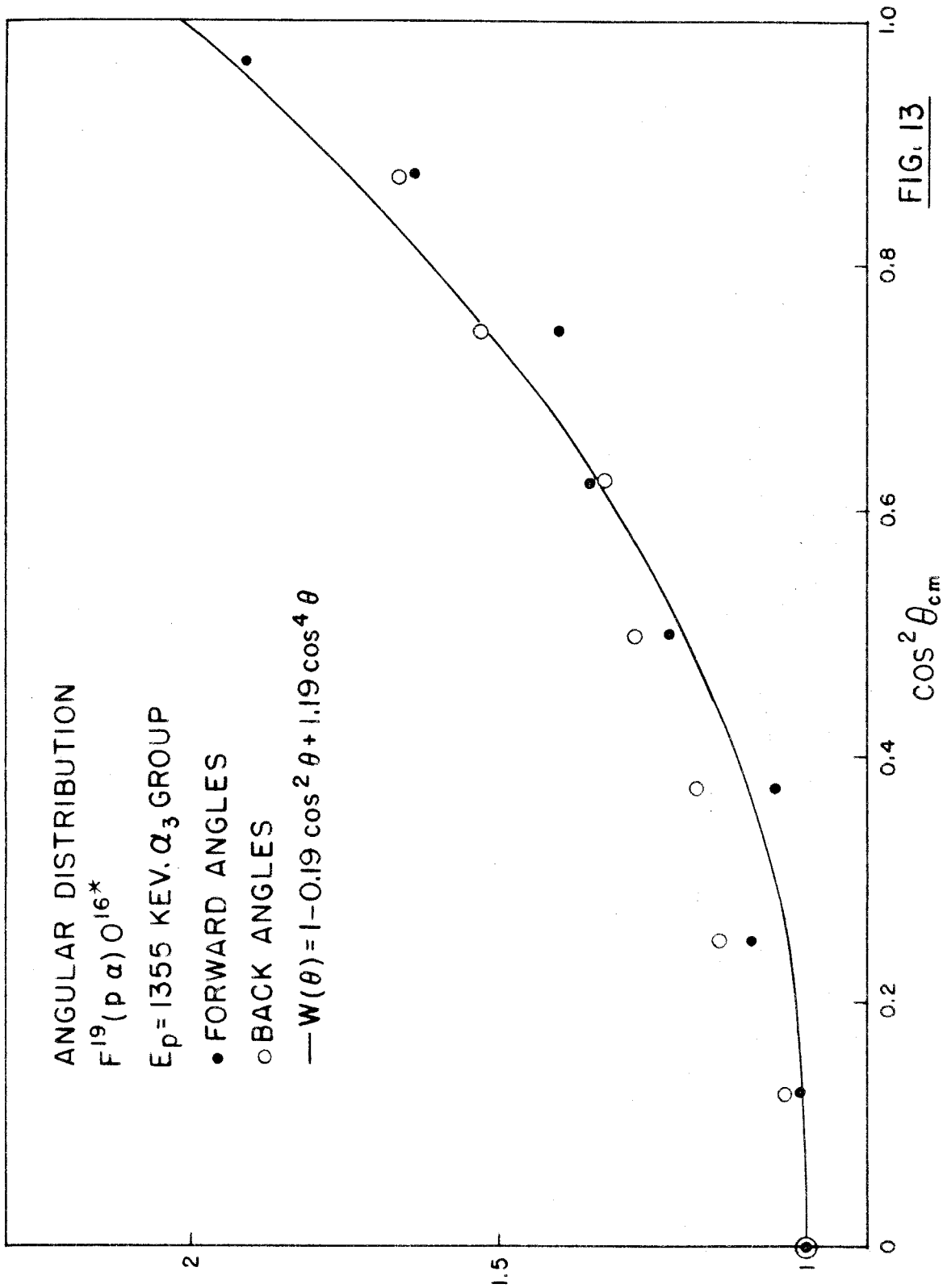
ANGULAR DISTRIBUTION
$F^{19}(p\,\alpha)O^{16*}$
E_p = 1355 KEV. α_3 GROUP
• FORWARD ANGLES
○ BACK ANGLES
— $W(\theta) = 1 - 0.19\cos^2\theta + 1.19\cos^4\theta$
2
1.5
1
0
0.2
0.4
0.6
0.8
1.0
$\cos^2\theta_{cm}$

FIG. 13

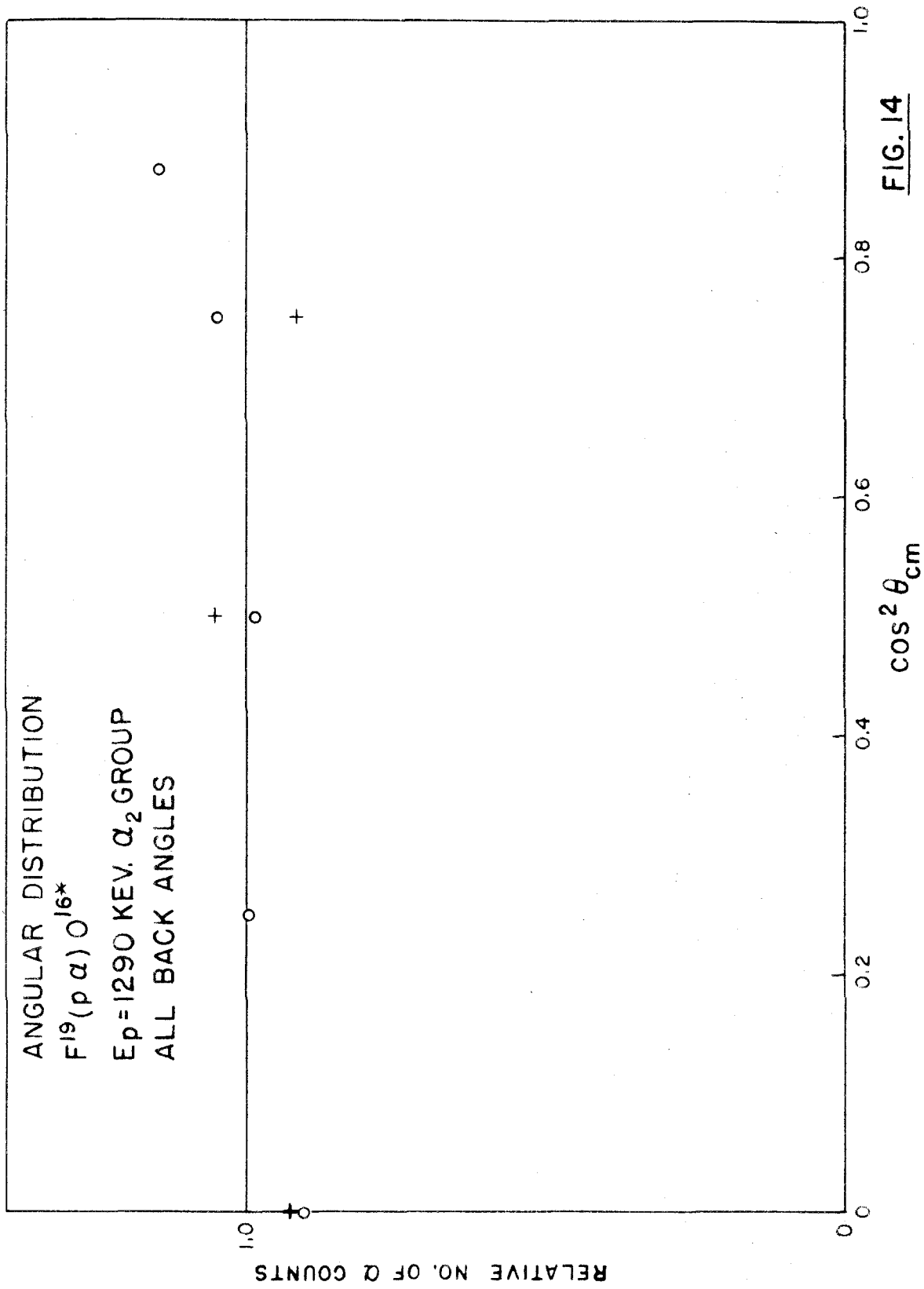
ANGULAR DISTRIBUTION
$F^{19}(p\,\alpha)\,O^{16*}$
E_p = 1290 KEV. α_2 GROUP
ALL BACK ANGLES
RELATIVE NO. OF α COUNTS
1.0
0
0.2
0.4
0.6
0.8
1.0
$\cos^2\theta_{cm}$

FIG. 14

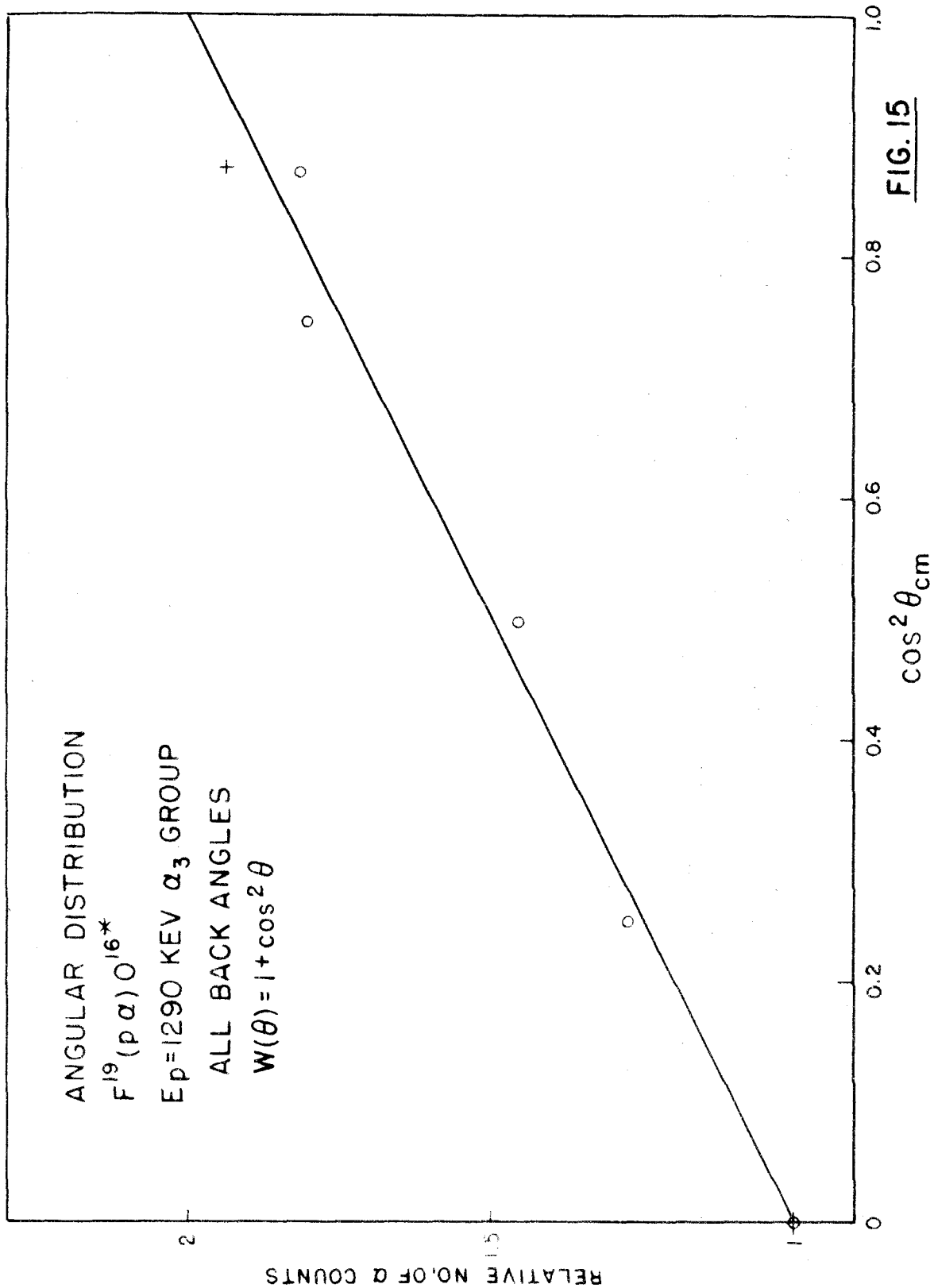
ANGULAR DISTRIBUTION
$F^{19}(p\alpha)O^{16*}$
Ep=1290 KEV α_3 GROUP
ALL BACK ANGLES
$W(\theta)=1+\cos^2\theta$
RELATIVE NO. OF α COUNTS
1
1.5
2
0
0.2
0.4
0.6
0.8
1.0
$\cos^2\theta_{cm}$

FIG. 15

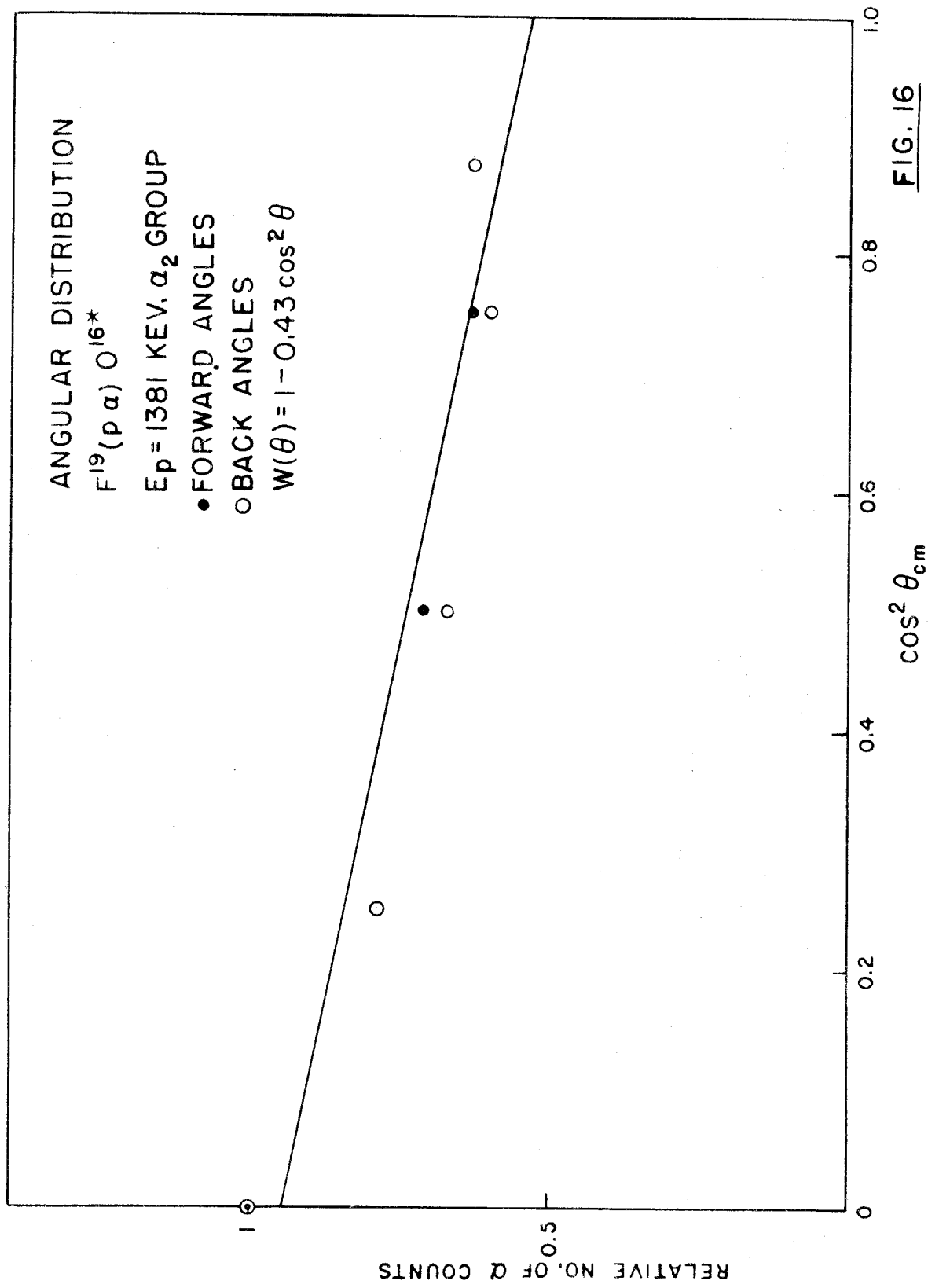
ANGULAR DISTRIBUTION
$F^{19}(p\,\alpha)\,O^{16*}$
E_p = 1381 KEV. α_2 GROUP
• FORWARD ANGLES
○ BACK ANGLES
$W(\theta) = 1 - 0.43\cos^2\theta$
RELATIVE NO. OF α COUNTS
1
0.5
0
0.2
0.4
0.6
0.8
1.0
$\cos^2\theta_{cm}$

FIG. 16

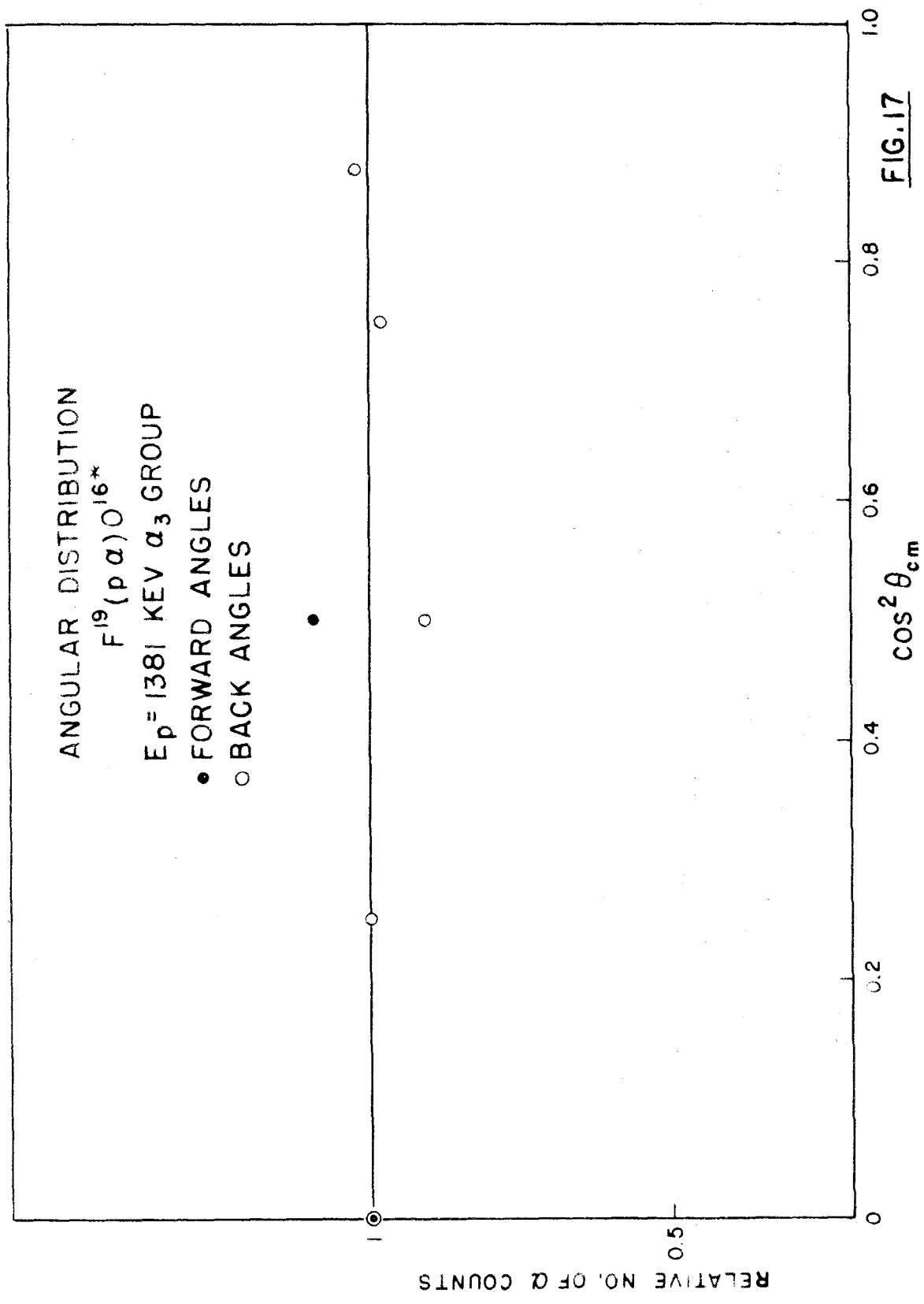
ANGULAR DISTRIBUTION
$F^{19}(p\alpha)O^{16*}$
E_p = 1381 KEV α_3 GROUP
• FORWARD ANGLES
○ BACK ANGLES
RELATIVE NO. OF α COUNTS
0.5
1
0
0.2
0.4
0.6
0.8
1.0
$\cos^2\theta_{cm}$

FIG. 17

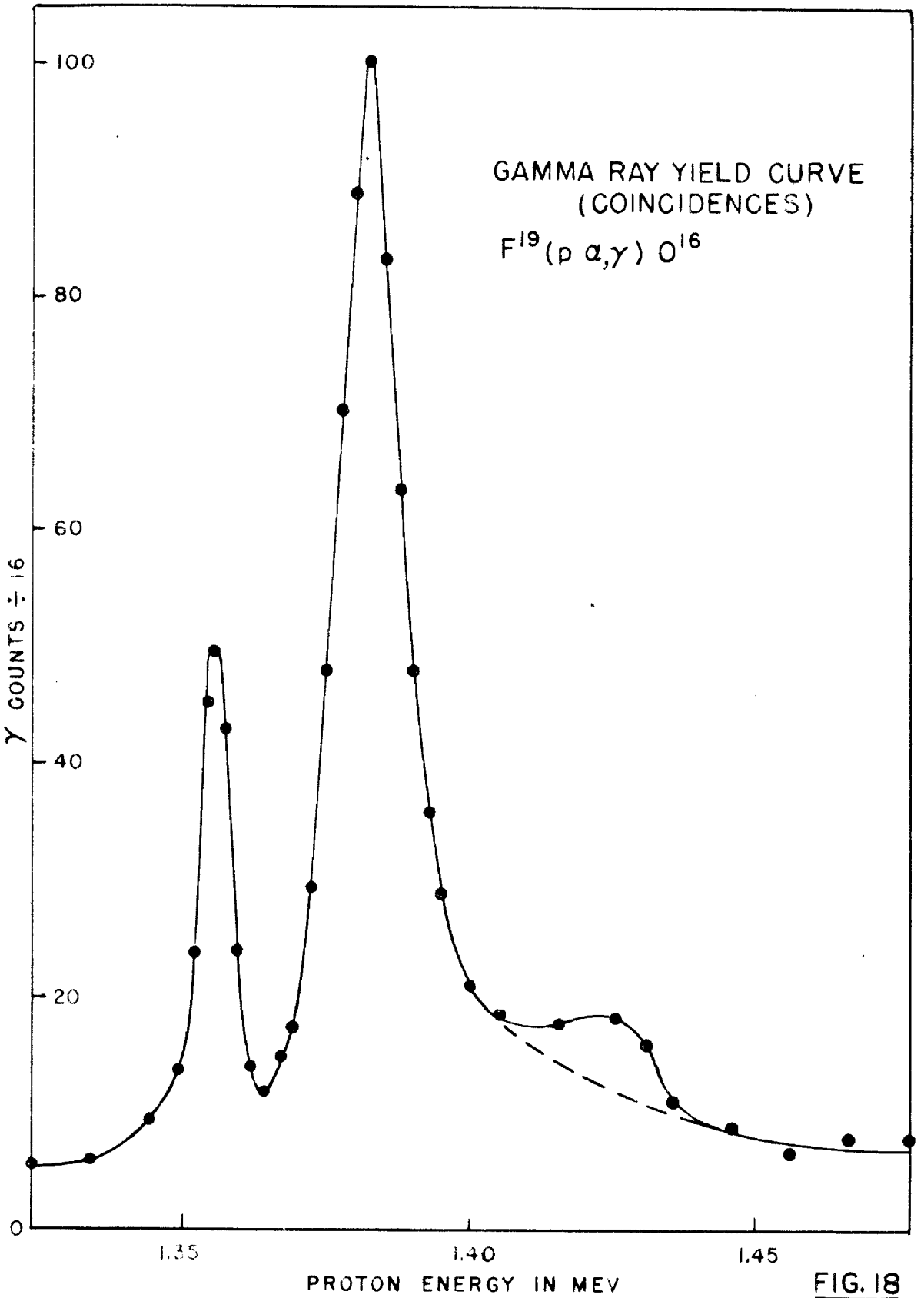
GAMMA RAY YIELD CURVE
(COINCIDENCES)
$F^{19}(p\,\alpha,\gamma)\,O^{16}$
100
80
60
40
20
0
γ COUNTS ÷ 16
1.35
1.40
1.45
PROTON ENERGY IN MEV

FIG. 18

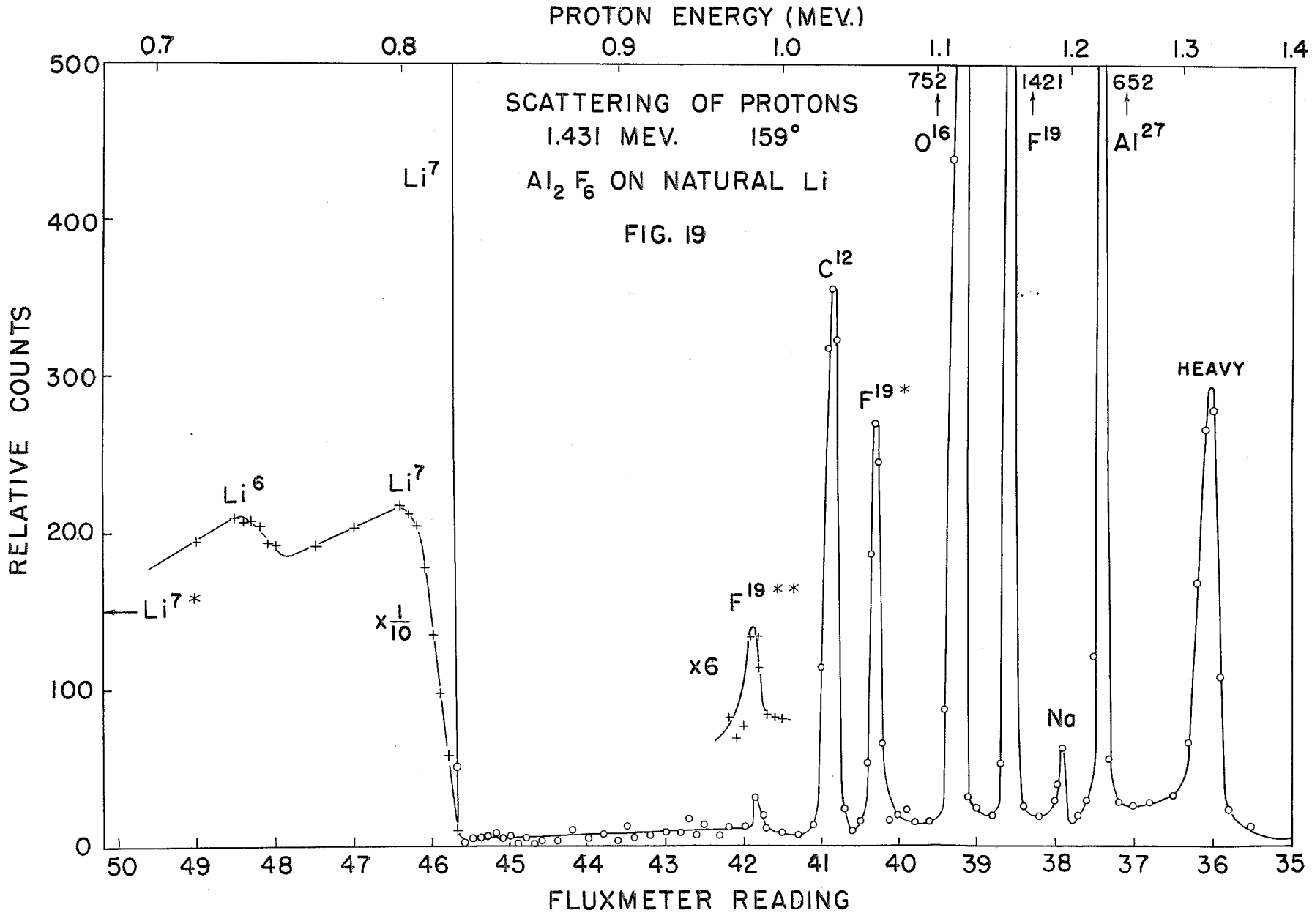
PROTON ENERGY (MEV.)
0.7
0.8
0.9
1.0
1.1
1.2
1.3
1.4
SCATTERING OF PROTONS
1.431 MEV. 159°
Al2 F6 ON NATURAL Li
FIG. 19
RELATIVE COUNTS
500
400
300
200
100
0
Li7
Li6
Li7
Li7*
x 1/10
F19**
x6
C12
F19*
752
O16
1421
F19
652
Al27
Na
HEAVY
50
49
48
47
46
45
44
43
42
41
40
39
38
37
36
35
FLUXMETER READING

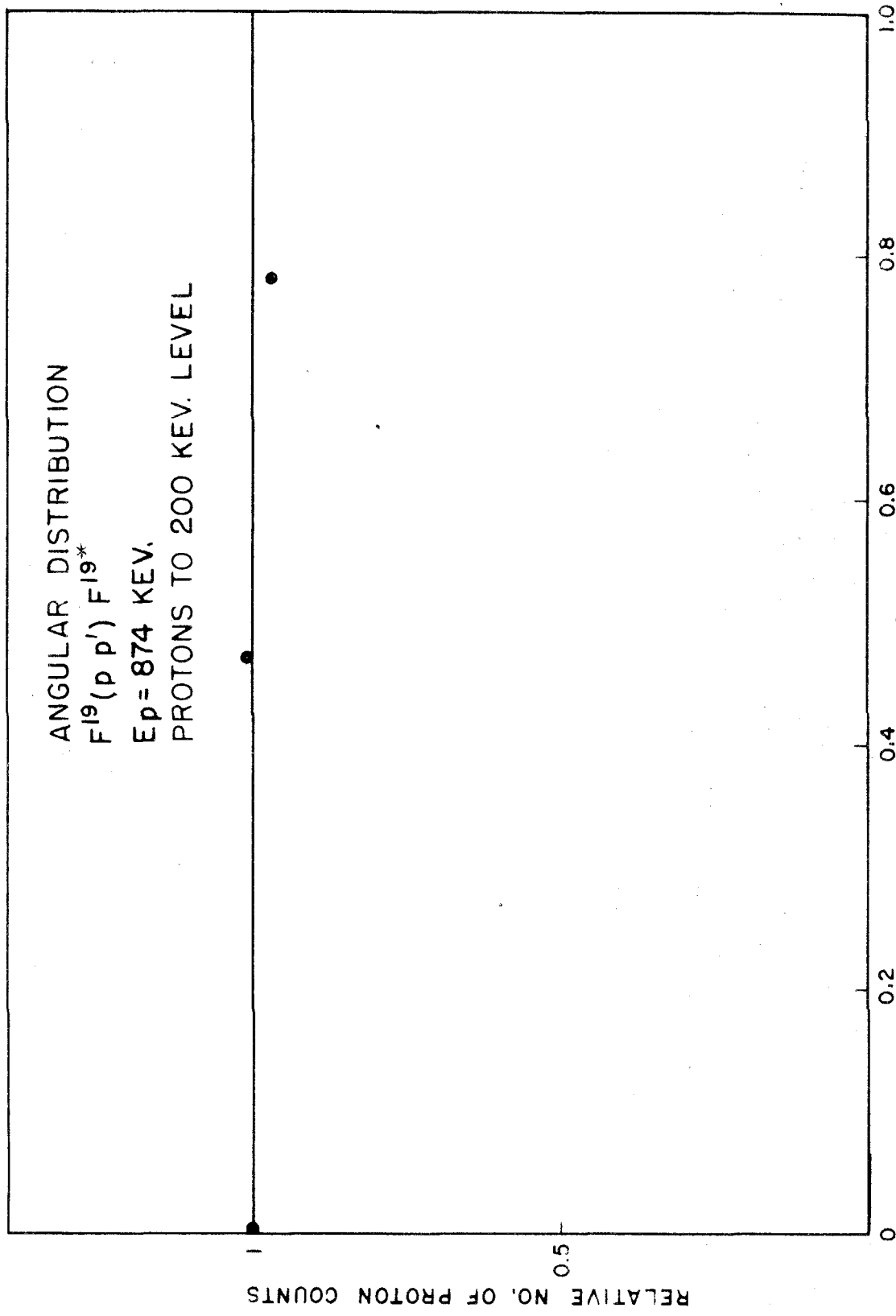
ANGULAR DISTRIBUTION
$F^{19}(p\,p')\,F^{19*}$
Ep = 874 KEV.
PROTONS TO 200 KEV. LEVEL
RELATIVE NO. OF PROTON COUNTS
1
0.5
0
0.2
0.4
0.6
0.8
1.0
$\cos^2\theta_{cm}$

FIG. 20

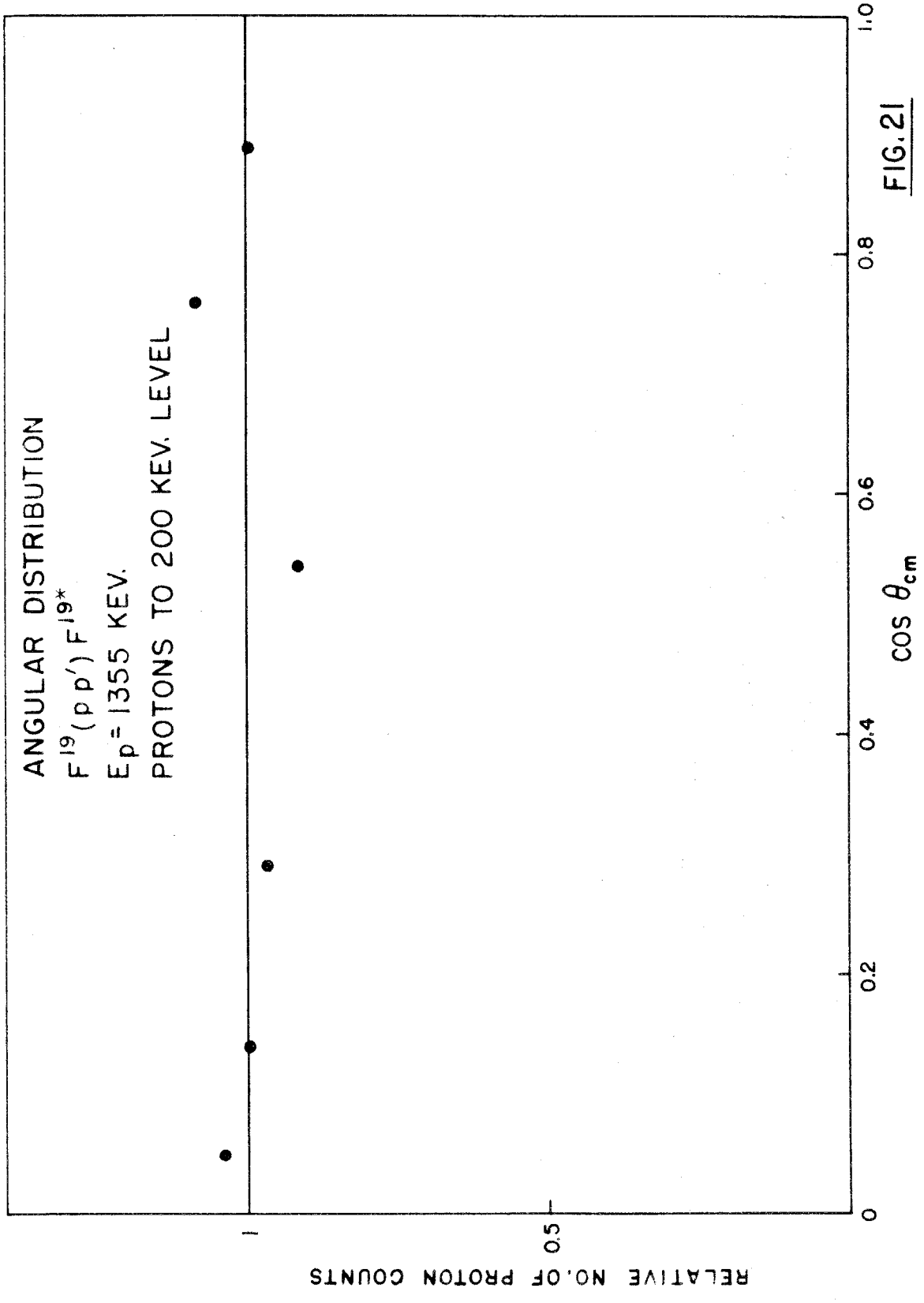
ANGULAR DISTRIBUTION
$F^{19}(p\,p')\,F^{19*}$
E_p = 1355 KEV.
PROTONS TO 200 KEV. LEVEL
RELATIVE NO. OF PROTON COUNTS
1
0.5
0
0.2
0.4
0.6
0.8
1.0
COS θ_{cm}

FIG. 21

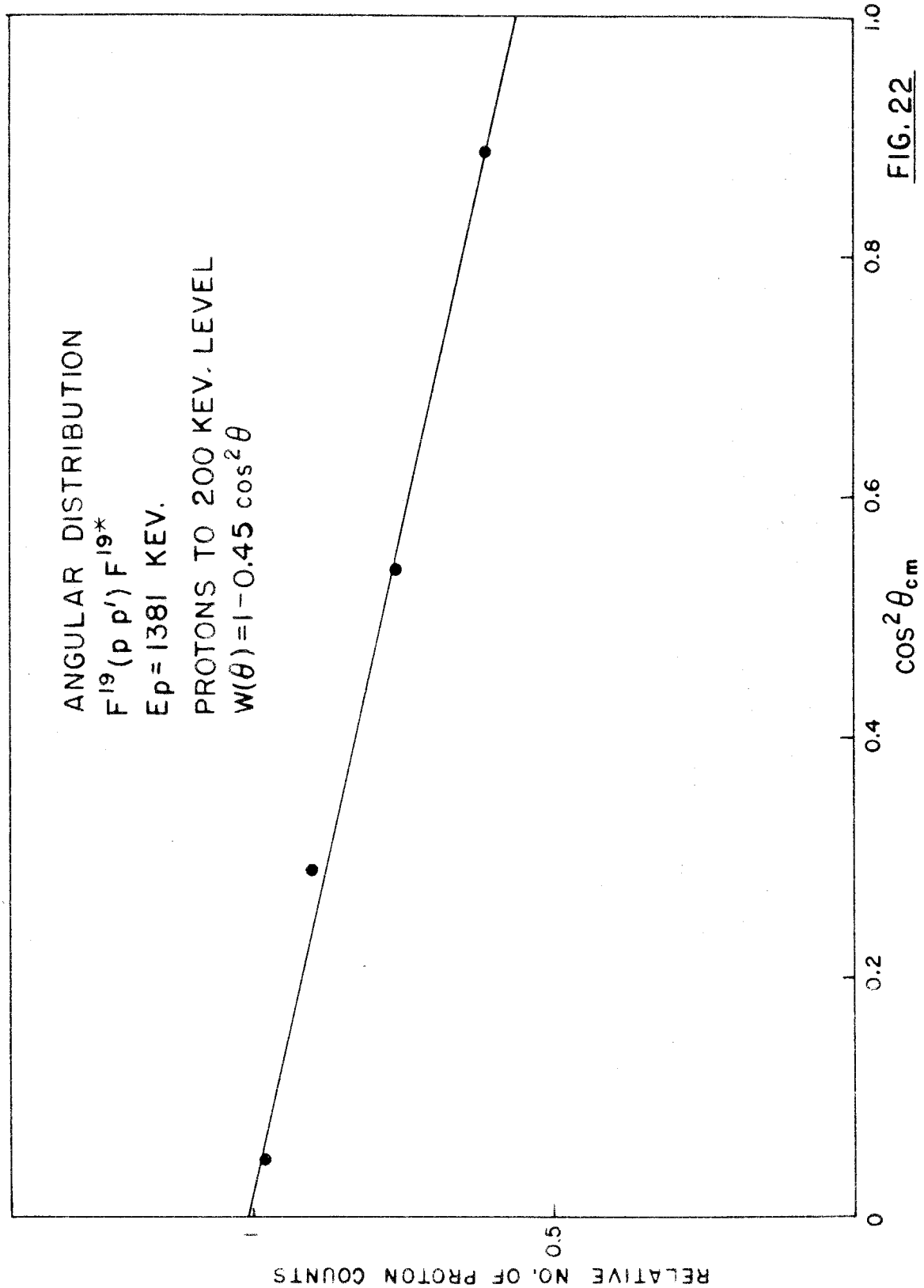
ANGULAR DISTRIBUTION
$F^{19}(p\,p')\,F^{19*}$
Ep = 1381 KEV.
PROTONS TO 200 KEV. LEVEL
$W(\theta) = 1 - 0.45\cos^2\theta$
RELATIVE NO. OF PROTON COUNTS
0.5
0
0.2
0.4
0.6
0.8
1.0
$\cos^2\theta_{cm}$

FIG. 22